ENERGY, ENVIRONMENT & STORAGE

AN INTERNATIONAL JOURNAL

Volume-4
Issue-2
May, 2024
ISSN: 2791-6197

ENERGY, ENVIRONMENT AND STORAGE

EES JOURNAL

Founded and Published by Erciyes Energy Association

Energy, Environment and Storage Journal is indexed in Crossref

Printed in Turkey

ISSN-2791-6197

EES- EDITORIAL BOARD

BOARD MEMBER

AIM AND SCOPE

Energy, Environment and Storage papers consider the prospects of energy technologies, environment, materials, process control and industrial systems. The Energy, Environment and Storage will be published 3 times per year.

Contributions describe novel and significant applications to the fields of:

- Hydrogen Fuels
- Hydrogen and Fuel Cell
- Hydrogen Economic
- Biomass
- Solar PV Technology
- Solar Thermal Applications
- Wind Energy
- Materials for Energy
- Drones and Energy Applications
- Nuclear Energy and Applications
- Hydro Power
- Fuel Technologies (CNG, LNG, LPG, Diesel, Gasoline, Ethanol, etc.)
- Numerical Modelling
- Energy Storage and Systems
- Battery Technologies
- Energy Management
- Heat and Mass Transfer
- Aerodynamics
- Aerospace and Energy Applications
- Combustion
- Electric Vehicle Transportation
- Off-grid Energy Systems
- Environment Management
- Air Pollution
- Water and Wastewater Pollution
- Water and Wastewater Management
- Waste Management
- Global Warming and Climate Change
- Environmental Ecosystem
- Environmental System Modelling and Optimization
- Ecological Applications or Conservation

VOLUME 4, ISSUE 2

MAY 2024

CONTENTS

Energy, Environment and Storage

Journal Homepage: www.enenstrg.com

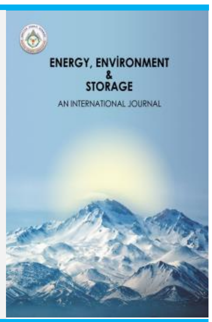

Effect of Excess Air Ratio on Emissions, Performance and Efficiency of Gasoline Fueled Engines: A Review

Happy Sinkala[1*], Saliha Özarslan[2], Abdallah Benarous[3,4]

[1]Graduate School of Natural and Applied Sciences, Mechanical Engineering Dept. Erciyes University, Kayseri, Türkiye

ORCID: 0009-0006-8871-6813

[2]Amasya University, Technical Sciences Vocational School, Automotive Program, Amasya, Türkiye

ORCID: 0000-0001-5696-9644

[3]Department of Mechanics, Technology Faculty, University Blida 1, Algeria

[4]LISICPE Laboratory, UHB University, Chlef, Algeria

ABSTRACT. This paper provides a comprehensive review of the fundamental impacts of excess air ratio (λ) on emissions and engine performance in spark-ignition engines. It examines pollutants such as oxides of nitrogen, unburned hydrocarbons, and carbon monoxide under both lean and ultra-lean conditions. In this paper, mainly the most prominent, up to date, and effective technologies such as ignition strategy, injection strategy, fuel blending, pre-chamber addition, are included. In addition to the effect the excess air ratio has on emissions, engine performance and efficiency are reviewed. This is done through the analysis of the Indicated Mean Effective Pressure, Coefficient of Variation, Fuel Consumption and Indicated Thermal Efficiency. The topics discussed relate to the primary categories listed above, but they are not exclusive to them. The paper concludes with a summary of findings and offers recommendations for future research directions..

Keywords: Guide, lean, emissions, performance, efficiency, fuel, combustion.

Article History: Received:27.03.2024; Accepted:17.05.2024; Available online: 31.05.2024

Doi: https://doi.org/10.52924/PUPX2065

1. INTRODUCTION

Fuel combustion has been widely used for many years to power transportation vehicles, produce electricity and heat for buildings and manufacturing operations. Nonetheless, given that energy cannot be produced, transported, or consumed without having a substantial negative influence on the environment, energy and environmental issues are tightly interlinked. Byproducts of fuel combustion, such as particulate matter (PM), carbon dioxide (CO_2), sulfur dioxide (SO_2), carbon monoxide (CO), and nitrogen oxides (NOx), have a negative impact on the environment. The poor quality of the air, the unprecedented climate change, and global warming are mostly caused by these pollutants. In an internal combustion engine, the burning of gasoline releases carbon monoxide, nitrogen oxides, and hydrocarbons.

A key environmental challenge today revolves around decreasing emissions from internal combustion engines while simultaneously enhancing fuel efficiency and engine performance. Numerous techniques, including better engine design, improved fuel characteristics, and enhanced combustion modes, have been employed to lower emissions and increase efficiency in engines.

One of the most important variables influencing engine exhaust emissions is the air-fuel ratio. The air-fuel ratio controls the amount of energy released, the amount of undesired pollutants generated during the process, and whether a mixture is combustible or not. Because of this, controlling the air-fuel ratio is still a top priority for engine control, particularly for the purpose of reducing exhaust emissions pollution [1]. Additionally, a three-way catalytic converter's performance depends on the quality of the mixture, therefore suitable control mechanisms are

*Corresponding author: hapsink@gmail.com

needed to comply with emission regulations [2]. Since precise air-fuel ratio control is the cornerstone of low-emission technology for gasoline engines, researches have been conducted on air-fuel ratio control techniques to optimize three-way catalyst emission conversion efficiency and comply with global emission legislation [3–17]. Compared to engines operating under stoichiometric conditions, lean burn engines require higher levels of air-fuel ratio stability and control for lean operation; otherwise, misfires will occur, affecting engine power, economy, and emissions [18].

Not only is the air-fuel ratio a critical parameter in an internal combustion engine or industrial furnace for pollution control but it is significant for the purpose of performance tuning as well. The air fuel ratio has a significant impact on the engine's power and fuel efficiency. In a gasoline engine, the lean air-fuel ratio yields the lowest fuel consumption. The primary cause is the abundance of oxygen, which allows the fuel to burn entirely and produce mechanical work. On the other side, rich air fuel mixtures yield the most power.

From the above literature review, one realizes that air-fuel ratio is a crucial and noteworthy metric or indication for regulating or fine-tuning engine performance and factors that are directly related to air quality and reducing pollution. This paper will cover a review of the influence of an excess air ratio on engine performance and pollutant emissions. Since further charge dilution, i.e. ultra-lean conditions, affects the flame propagation speed, leading to combustion instability, different techniques used to overcome these limits and achieve a more stable combustion are mentioned. At stable ultra-lean combustion, the emission and performance characteristics of the engine are discussed.

2. EFFECT OF EXCESS AIR RATIO ON EMISSIONS, PERFORMANCE AND EFFICIENCY UNDER LEAN COMBUSTION

2.1 Effect of excess air ratio on emissions

The in-cylinder temperature, the air and fuel homogeneity, and the combustion mode all have a significant impact on emissions [19, 20]. Compared to SI mode, there are more emissions of CO and HC in HCCI mode. This is caused by trapped crevice gases, low in-cylinder temperatures, and incomplete oxidation brought on by the rapid combustion process. SI engines have higher NOx emissions than other engine types [20, 21]. It has been discovered that the HC and CO emissions in HCCI are primarily dependent on engine load, regardless of the air-fuel ratio. Engine speed has a smaller effect on CO emissions than it does on HC emissions [20].

Due to the sensitive nature of NOx generation to in-cylinder temperature and oxygen availability [22, 23], NOx emissions increase with in-cylinder conditions as well as fuel and air homogeneity, improved combustion, and better air/fuel mixing (λ=1.0 to 1.2). By burning fuel with an excess of air compared to the stoichiometric amount required for combustion per unit mass of fuel, it's possible to reduce in-cylinder temperature, thus leading to lower NOx emissions [24]. Conversely, a more diluted mixture cools the fresh charge and reduces the fuel rate even further, thereby reducing the heat release, average combustion temperature and deteriorates auto-ignition. Due to the considerably colder new charge, reduced fuel rate also results in incomplete combustion of HC and CO to CO_2 and low post-oxidation temperatures for the fuel/air mixture. HC and CO levels rise as a result [20, 25-26].

Ceviz et al. [28] investigated how engine emission characteristics were affected by an excess air ratio under lean operating conditions. According to their studies, at λ=1.2, an increase in the air excess ratio significantly reduced exhaust emissions relative to stoichiometric conditions by roughly 85% and 23% for CO and HC emissions, respectively.

Soot production is another emission where the excess air ratio has a major influence. When lean homogeneous combustion occurs at a higher thermal efficiency (excess ratio of about 1.2), less fuel film forms on the piston head, which results in low PM concentration [29]. However, as the air is diluted, i.e. further increasing the excess air ratio, the reduction in both the temperature and released heat, and an increase in combustion phase, limits the oxidation of the soot. For this reason, increasing the excess air ratio above 1.4 shows a re-increase in the PM concentration [29].

2.2 Effect of excess air ratio on performance and efficiency

As indicated in the previous section, the excess air ratio showed to have an effect on the emissions. Likewise, the effect of excess air ratio is observed in engine efficiency and performance. The range of λ in which the correct mixture burns in typical spark-ignited engines is relatively small. Engine performance becomes unstable when the fuel mixture is reduced to the point that the excess air ratio value is greater than 1.5. This can lead to a variety of issues, including misfiring and a non-repeatability of engine cycle.

The indicated mean effective pressure (IMEP) is one of the primary factors defining the performance of an internal combustion engine. The test engines indicated mean effective pressure decreases as the value of λ increases, resulting in a decline in performance caused by the deterioration of the excess air ratio mixture [26, 30]. The reported findings by M. Kumar and T. Shen [31] demonstrate this with the maximum pressure decreasing as the excess air ratio increases throughout all operating conditions. Lowering the fuel levels causes the in-cylinder temperature to drop [31], which in turn causes the pressure to drop, hence Pmax decreases.

The coefficient of variation in indicated mean effective pressure (COV_{IMEP}) is a useful tool for measuring and expressing engine work instabilities, which are related to the macro-scale combustion process. By calculating the IMEP from successive engine work cycles, the COV_{IMEP} is found. The value of the COV_{IMEP}, which indicates the variation in combustion stability, rises as the excess air ratio expands [30, 32].

When the combustion stability is achieved, the Indicated Specific Fuel Consumption (ISFC) typically drops because there is less pumping loss as the extent of lean conditions rises. Other variables, on the other hand, might have an impact on ISFC, which might rise in certain circumstances. Park et al. [25] reported that the ISFC increased in the intermediate range of operating circumstances i.e. λ= 1.4 and 1.6. It's probable that the fuel injected early in the process caused moisture on the walls, leading to a film of fuel on the piston and cylinder surfaces. The increase in Total Hydrocarbon (THC) emissions might stem from some of the fuel injected early not fully engaging in combustion. Additionally, because of better fuel evaporation and air usage, a higher injection pressure was better for fuel efficiency. Nevertheless, owing to the cylinder receiving a lesser amount of energy i.e. fuel, the engine performance decreases. The ISFC is affected by the combustion phasing in a manner similar to the COV_{IMEP}, which is dependent on the ignition timing [26].

Under varying engine loads, equivalent brake specific fuel consumption (BSFC) decreases. However, the increasing λ reduces BSFC only up to a certain minimum, then it subsequently increases BSFC. For the different tested fuels, this was reported [23, 33], and according to the authors [23], the following variables might have contributed to this. First, when λ increases, the engine load was maintained by increasing the throttle opening angle and boosting the intake manifold pressure. This lowered the peak combustion temperature and, as a result, less heat is lost through the combustion chamber walls and less pumping work is required. In the meantime, increased intake pressure raises the fuel-air mixture's heat capacity ratio in the cylinder, enhancing the engine cycle's thermal efficiency. As a result, the equivalent BSFC decreases. However, when λ is increased to 1.5, poor constant-volume combustion and high air dilution rate cause misfires, which lower thermal efficiency and increases equivalent BSFC.

As was already mentioned during the combustion phase, the influence of air dilution on combustion increases the rate of misfires as well as the emissions of THC and CO, which lowers the value of total heat release and ultimately lowers thermal efficiency. Moreover, because of the poor combustion performance, this behavior will be notable at large λ. Conversely, the efficiency of combustion increases when the combustion phenomenon achieves stability thanks to better combustion and improved air- fuel mixing, after which it decreases as λ increases. Additionally, there is sufficient fuel as well as oxygen in the mixture for adequate oxidation (air-fuel mixing), which means that when more fuel oxidizes, there will be just a little excess of oxygen available.

Moreover, when λ increases beyond 1.4, there is insufficient fuel in relation to the excess oxygen present in the cylinder. This results in an improperly mixed mixture, or heterogeneous mixture, and hinders the smooth propagation of the flame front, causing partial combustion or misfires. These occurrences indicate the instability of the combustion phenomenon with lean-zone combustion and, ultimately, a decrease in combustion efficiency [26, 31].

In their study of the impact of excess air ratio on cyclic variability and engine performance characteristics under lean operation conditions, Ceviz et al. [28] concluded that lean burn combustion spark ignition engines can offer notable advantages in low load conditions, particularly when the engine is well-designed and the air-fuel mixture formation strategy is optimized. Under such circumstances, thermal efficiency increases by approximately 30%. However, specific fuel consumption and HC emissions start to increase once the excess air ratio exceeds around λ = 1.25. This also resulted in a more rapid increase in cyclic variability.

From the findings and as shown in table 1, it can be seen that increasing the fuel air ratio even further, or achieving ultra-lean combustion, may help the engine and power industries comply with the strict emission rules pertaining to nitrogen oxides (NOx). However, when λ grows from 1.4 onwards, the in-cylinder combustion phenomenon exhibits instability characteristic [23]. Additionally, inadequate ignition caused by a more diluted mixture can cause misfires in the engine. Misfires and ignition problems like these can cause rough operation, cycle-to-cycle variability, efficiency reduction, and an increase in emissions of unburned hydrocarbons. The narrow flammability limit will also restrict the NOx reduction.

In order to attain a short burn duration and good combustion stability in ultra-lean combustion, a number of attempts have been undertaken to provide a reliable ignition process and to improve fuel oxidation. The next sections review the different combustion and ignition techniques and works carried out to extend the excess air ratio and the effect it has on emissions, engine performance and efficiency under ultra-lean conditions.

Table 1 Summary of the effect of excess air ratio (lean burn) on performance, efficiency and emission characteristics

Author	Operation	Performance & Efficiency	Emissions
C. Park et al [25]	For a single injection, a lean mixture was formed. Engine speed of 3000 r/min Indicated mean effective pressure of 0.4 MPa Fuel injection pressure ranging from 10 MPa to 20 MPa.	Under lean burn - The Indicated Specific Fuel Consumption decreased owing to the reduced pumping loss - Possibility of misfire to occur as λ.	Due to further increase λ i.e. in lean burn - NOx decreased - THC emissions increased - the opacity increases
A. Jamrozik, W. Tutak [26]	A traditional, single-stage combustion process, Air-fuel mixtures with excess air ratios (λ) are managed appropriately, ensuring they do not exceed 1.5.	- λ goes beyond 1.5, misfire and non-repeatability of engine cycles occurred and engine efficiency decrease	At λ greater than 1.2 - NOx decreased At λ less than 1.5 - Both HC and CO decreased
C. Park et al [29]	The test parameters were set to 2000 rpm and 0.2 and 0.4 MPa for the brake mean effective pressure, in each case. The test settings included a spray-guided direct-injection system to ensure lean combustion.		-At λ about 1.5, the Particulate Matter (PM) increased dramatically - Increasing λ to higher than 2.0 leads a re-increase in the Particulate Matter concentrations
Martinez S [30]	The engine was run during the intake stroke at a fixed rotational speed of 1000 rpm, with the throttle wide open. The maximum brake torque setting for each case was taken into consideration when choosing the spark timing, and the excess air ratio was increased from 1 to levels that were almost at the flammability limit.	- When implementing lean combustion, IMEP dropped as λ increased. - Stable engine operation was maintained with COV values below 4% until λ = 1.5. Following this, there was a sharp rise in instability, peaking at about 6%. - Up to λ = 1.5, fuel conversion efficiency increases	-Emissions were not covered in the study
M. Kumar, T. Shen [31]	A traditional gasoline engine of the V6 type equipped with two fuel injection systems.	- As λ rises, less heat is released. - Combustion efficiency increases till λ = 1.4 and then decreases with additional λ increases -In-cylinder pressure decreases	- Because of improved combustion efficiency, NOx emission initially increases about λ=1.1 to 1.2 and then decreases as λ increases further.
Ceviz et al [28]	The engine speed 2500 rpm, at thirteen (13) different air-fuel ratios	- There is a noticeable decline in combustion quality as one approaches the lean operating limit. - Up to λ = 1.3, an increase in λ caused the cyclic variations to increase approximately linearly. The rate at which the cyclic variations increased after this value was extremely rapid. - Up to λ = 1.2, the specific fuel consumption reduced and the thermal efficiency increased as λ increased.	- CO emissions decreased (85%) dramatically down to λ =1.1 and continued to decrease as λ increased. - CO_2 emissions decreased linearly with the increase λ - HC emissions decreased (23%) up to λ =1.25, and started to increase after this point. - NOx emission reached maximum at λ =1.1. After this value, NOx emission decreased linearly
C.-W. Wu et al. [55]	A typical engine was used to evaluate ethanol–gasoline-blended fuel at different air-fuel ratios (λ).	- When the λ ratio is marginally less than one, the maximal torque output is attainable at all throttle valve openings. As λ increases, the cylinder's combustible vapor content decreases, resulting in a decrease in torque output.	For 100% pure gasoline fuel: - As λ approaches unity, CO emissions decrease, and may even reach zero under lean conditions. - At λ slightly larger than one, the amount of HC emission is minimum, owing to complete combustion. - With further increases, such as when λ surpasses 1.4, the level of HC emissions rises due to combustion becoming highly incomplete.

3. EFFECT OF EXCESS AIR RATIO ON EMISSIONS UNDER ULTRA-LEAN COMBUSTION

3.1 Ignition and Injection Strategy

The lean-burn limit is influenced by both the injection method and the ignition timing, as the latter determines the combustion phase. In lean operation conditions, late injection is effective than early injection at ensuring stable combustion with sufficient mixture formation. [2, 34-35]. With late injection, however, it is challenging to reduce the misfire tendency due to the huge amount of fuel injected under mid-load operating conditions. By utilizing converging-diverging nozzles with a specific aspect ratio in the pre-chamber, a supersonic hot jet technique allows combustion engines to burn ultra-lean mixtures. Increased fuel economy, decreased NOx emissions, and improved combustion efficiency are all shown benefits of supersonic jet ignition [36–19]. Additionally, it was noted that, in comparison to homogeneous combustion, the lean-burn limit was noticeably extended for stratified operation [37, 38]. In their study of the in-cylinder air-fuel ratio control problem for the lean burn mode of SI engines using cycle-based mode, Kumar et al. [31] discovered that stable combustion at an excess air ratio significantly extended to λ=2 can be achieved by fuel split injection, which enables the formation of an adequate stratified mixture in lean combustion conditions. The findings also indicate that combining lean combustion with intake tumble holds significant promise for conserving energy and reducing emissions in gasoline engines. Fig. 2 shows a continuous drop in CO_2. Experiments conducted by F. Zhou et al. [39] demonstrate that utilizing intake tumble notably extends the lean combustion limit while maintaining acceptable combustion stability. This approach increases the indicated thermal efficiency by 7.2% compared to the engine's initial state without tumble (at λ = 1), while the particular emissions of CO_2, CO, HC, and NOx can be decreased by, at most, 85.3%, 72.2%, 12.0%, and 5.8%, respectively as illustrated in figures 1, 2 and 3.

Microwave ignition has been shown to significantly increase the internal combustion engine's lean-burn limit [40]. The lean limit was demonstrated by Hwang et al. [41] in their experiments with the conventional spark ignition system at λ =1.28; however, the lean limit was extended to λ=1.57 by the microwave-assisted plasma ignition system. It was also proven that the air/fuel ratio is the main factor influencing CO emissions from internal combustion engines. Regardless of the ignition mode, as the lambda was increased, the CO emissions reduced. Simultaneously, a considerable decrease in CO emissions was found upon microwave activation. From Fig. 1, at a lambda value of 1.0, the CO emission dropped to 0.11% with microwave-assisted plasma ignition (520mJ) as opposed to 0.35% with traditional spark ignition. Microwave aided plasma ignition cut CO emissions by approximately 49% under lean operating conditions. Under lambda 1.0 conditions, the HC emissions from microwave-assisted plasma ignition (520mJ) and traditional spark ignition are 3108 ppm and 5175 ppm, respectively (Fig. 3). Furthermore, in lean operational settings, microwave-assisted plasma ignition could potentially reduce HC emissions by approximately 29%. This is attributed to the increased temperature and accelerated flame velocity generated by the microwave-assisted plasma ignition. Conversely, depicted in Figure 4, NOx emissions from the microwave-assisted plasma ignition system surpassed those from the conventional spark ignition setup due to the higher in-cylinder temperatures. In a lean condition, the average rate of growth in NOx emissions was 115%.

3.2 Prechamber addition

The gasoline pre-chamber allows for the creation of ultra-lean mixtures with dilution ratios up to λ = 2.1. Similarly, burning of lean gas-air mixtures with an excess air ratio above the value of 1 (up to about 1.8) was obtained in the investigation of a two-stage combustion system [19]. Under these extremely lean circumstances, the NO_2/NOx ratio is almost 100% in terms of emissions [42]. When using a NOx storage catalyst, the high NO_2 to NOx ratio is advantageous.

Based on a SI stationary engine using a two-stage LPG-powered combustion system, Jamrozik et al. [26,43] discovered that the test engine's Air-Fuel mixture stratification method allowed lean mixture to burn with an overall excess air ratio of up to 2.0 thanks to the two-staged combustion system with pre-chamber. The centrally positioned active pre-chamber that allowed for independent regulation of the air/fuel ratio in the main combustion chamber facilitated the achievement of stable ignition and rapid flame propagation. Operating at an excess air ratio of up to 2.0, in turn, reduced NOx emissions from the exhaust as illustrated in Fig. 4.

3.3 Spark Discharge Interval

In SI engines, combustion initiation occurs through the spark discharge generated between the electrodes of the spark plug [44-46]. This discharge forms a high-temperature plasma kernel around the spark plug, facilitating the transfer of energy from the plasma to the combustible mixture. Subsequently, this initial flame kernel then becomes the propagating flame [32, 47]. According to Jung et al. [48], a rapid tumble motion in conjunction with a high discharge energy can further extend the lean limit, increasing maximal efficiency and lowering emissions. Under lean conditions, the longer discharge interval decreases the Cycle-to-Cycle Variation (CCV) of combustion, and Tsuboi et al. [49] indicated that achieving an operation at λ=2.3 was possible with a discharge interval of 0.4ms. However, their study highlighted that excessively long or short intervals between spark discharges lead to unstable lean operation, characterized by significant cycle-to-cycle variability in SI combustion, particularly for ultra-lean SI operation at λ ≈ 2.0. As consequence, an understanding of the phases of spark discharge is particularly important to find an optimum interval between spark discharges to minimize variations in combustion and ultimately increase the lean-stability limit. Nakata et al. [50] reported a similar finding, observing that the lean limit at a discharge current of 300 mA was extended to an excess air ratio of 1.96 due to the larger discharge current or longer discharge duration. According to Astanei et al, when comparing the efficiency of double spark plugs in enhancing the performance of combustion engines, the energy that the double spark plug (DSP) delivers to the discharge during long pulse durations is 20% more than that of the conventional spark plug. It was noted that even at equivalency ratios in the region of 0.65, where the usage of conventional spark plug (CSP) tends to cause misfires and extremely significant engine vibrations, the DSP can offer more stability for such very lean mixtures [51]. The high discharge stabilizes the initial stage of combustion by producing a large flame. Since the initial stage of combustion controls all combustion in a SI engine, a stabilized kernel flame forms quickly, which shortens the initial flame growth period and allowed for a decrease in combustion variations, which are represented by the CVV. [52, 53]

3.4 Fuel Blending

The use of the methods above, standalone or combined would greatly increase combustion stability under ultra-lean conditions. Other than that, the use of blended fuels, gasoline and ethanol for example, can enhance the combustion rate. In his research, Xiumin Xu [21] showed that the highest indicated thermal efficiency of ethanol/gasoline blends is higher than that of ethanol by 0.4% and 8.8%, respectively, at λ=1.2 and λ=1.4. Based on these findings, the EPI+GDI mode performs better in lean burn conditions.

A similar situation was seen in the LPG+Gasoline blending case [26, 43], where a pre-chamber Gasoline+LPG mix injection allowed for higher air ratio operation at high thermal efficiency.

Lower nitrogen oxide emissions were seen in the engine's exhaust gas after burning an ultra-lean mixture with an overall excess air ratio of up to 2.0 in the test engine. It did, however, result in a rise in hydrocarbon and carbon monoxide levels as shown in Fig. 1 and Fig. 3. It has already been demonstrated that using a leaner air fuel ratio and an appropriate catalytic converter can greatly reduce CO and (HC + NOx) emissions [54].

The performance and emissions of a conventional engine using gasoline-ethanol blended fuel were investigated by C.-W. Wu et al. [55] at different air-fuel ratios (λ). It was demonstrated that when the blended fuel's ethanol percentage increased, and as a result of oxygen enrichment, CO and HC emissions decreased. The highest quantities of CO_2 and the smallest amounts of CO and HC were obtained at an air-fuel ratio that was marginally larger than one. It was observed that the air-fuel ratio controlled CO_2 emission during lean combustion conditions, whereas CO_2 emission is compensated by CO emission under rich combustion conditions. It was also discovered that blended fuels had CO_2 emissions per unit horse power output that were either comparable to or lower than those of gasoline fuels.

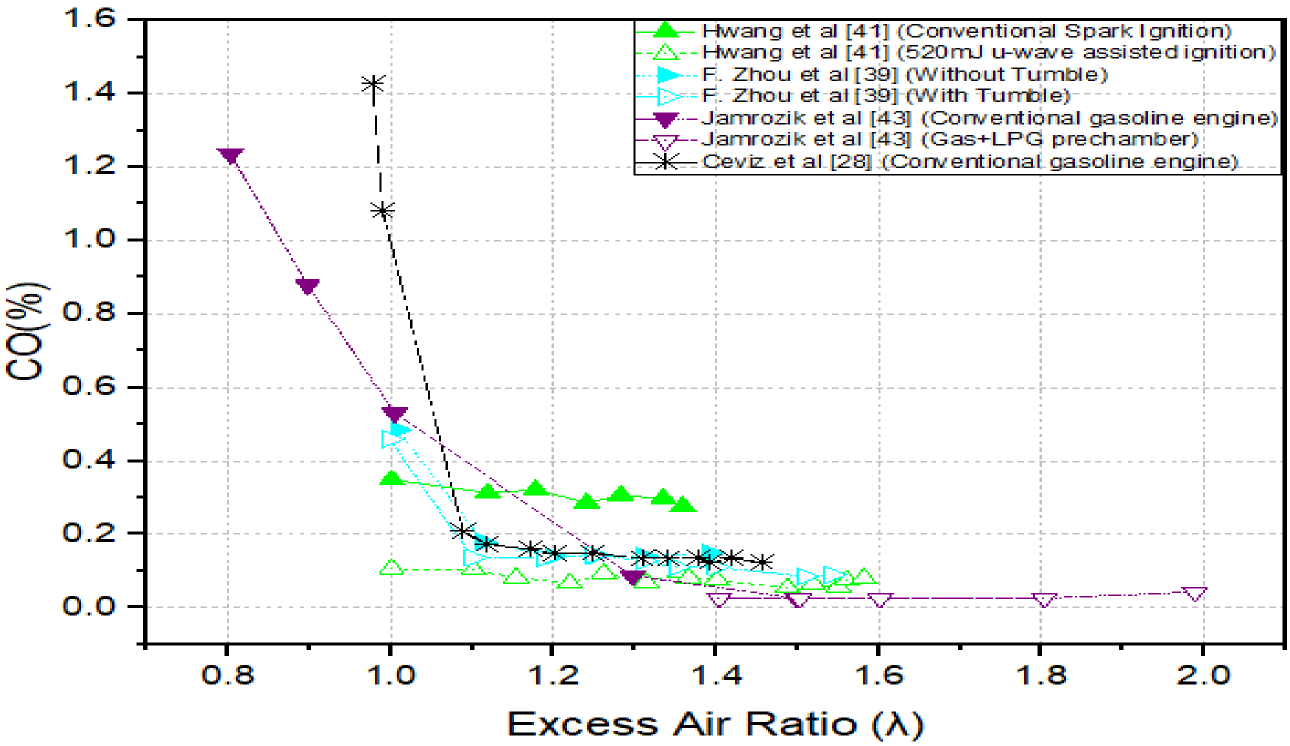

Fig. 1. The effect of excess air ratio on CO emissions

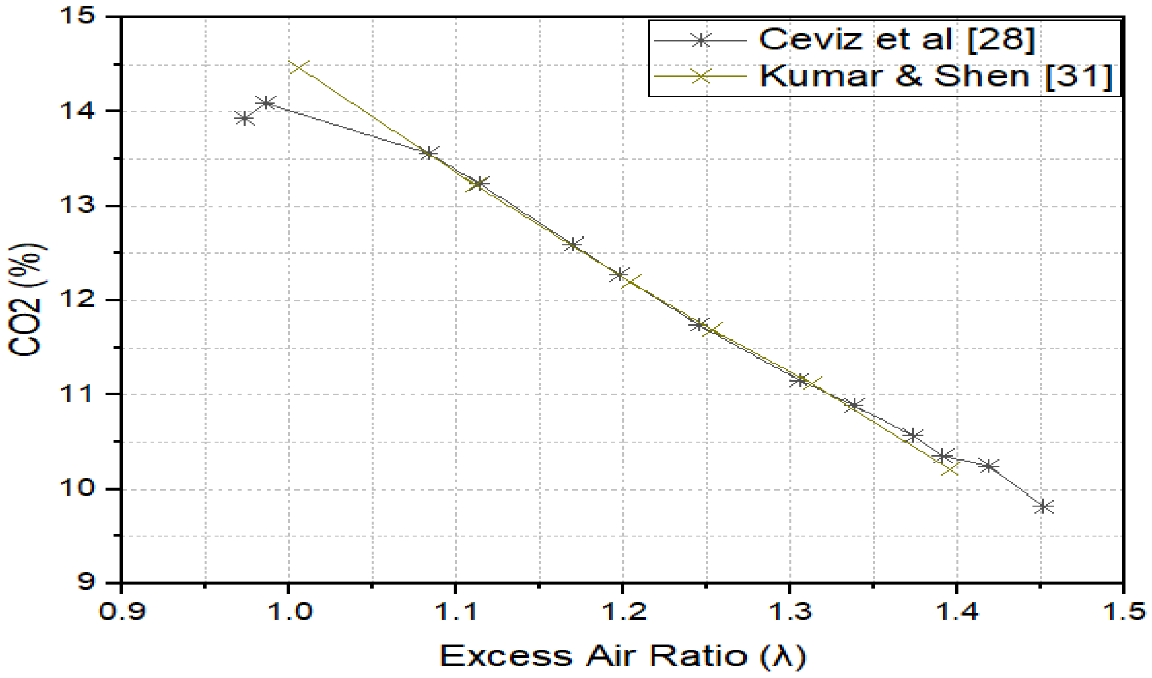

Fig. 2. The effect of excess air ratio on CO_2 emissions

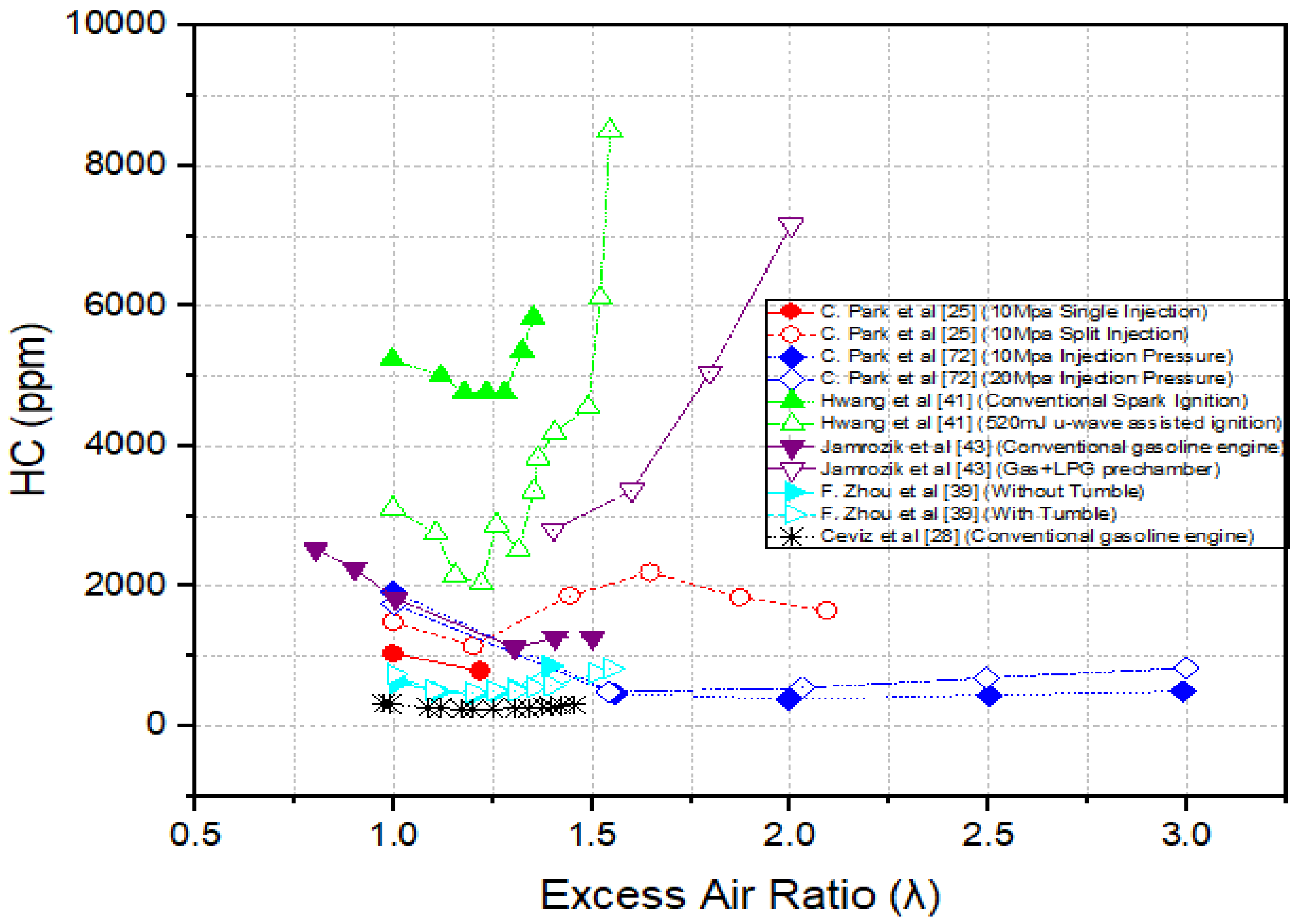

Fig. 3. The effect of excess air ratio on HC emissions

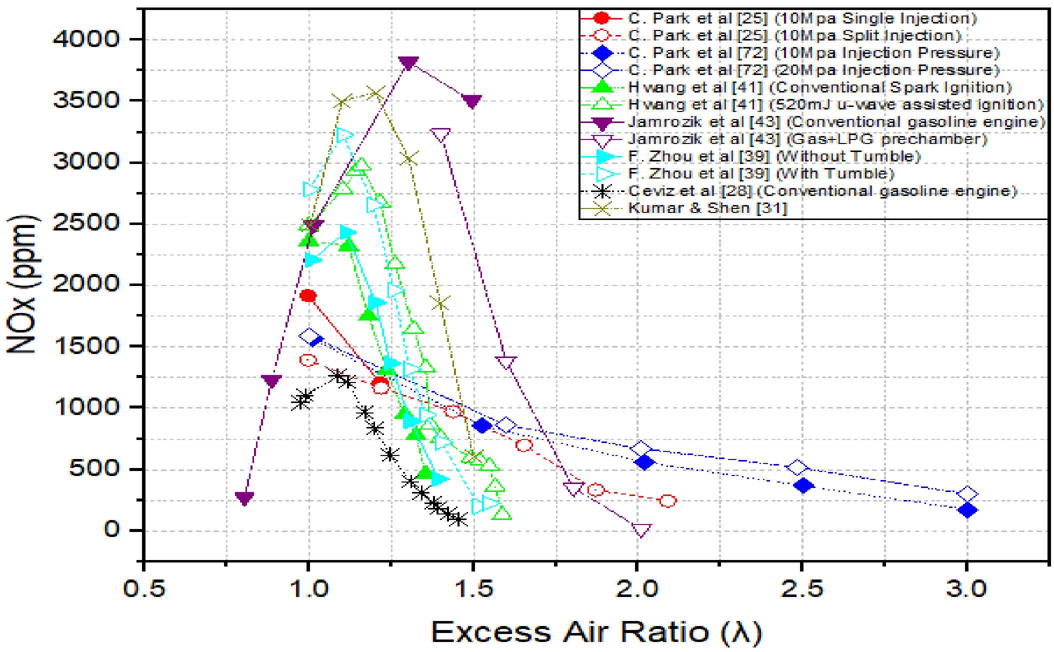

Fig. 4. The effect of excess air ratio on NO_X emissions

4. EFFECT OF EXCESS AIR RATIO ON PERFORMANCE AND EFFICIENCY UNDER ULTRA-LEAN COMBUSTION

Improving of efficiency and performance requires an expanded stable combustion range. Modern gasoline engine design aims to optimize efficiency and fuel economy while minimizing emissions to comply with regulations. Strategies such as downsizing, maximizing tumble flow, and increasing exhaust gas recirculation rates have shown to be effective [56-58]. Yet, there's still a need for ongoing improvement in engine designs and components to fully leverage these advantages. In particular, the ignition system has been an important aspect in the application of these strategies.

4.1 Microwave ignition

Numerous studies have summarized the fundamentals of plasma ignition and aided combustion [59–64], and it has been shown that microwave ignition significantly improves lean-burn mixed ignition performance [53, 65-66]. The utilization of microwave plasma ignition and assisted combustion technology results in a uniform distribution of flame intensity, increased propagation speed, enhanced combustion efficiency, extended lean burn flammability limits, and decreased emissions of pollutants. Moreover, multi-point ignition and stable combustion are achieved.

In comparison to a spark plug, a Multiple Microwave Discharge Igniter (MDI) operating as a 2point or 3point igniter significantly improved lean limit performance [58Hwange et al. [41] investigated the utilization of a novel microwave-assisted plasma ignition system in a direct injection gasoline engine. Their study revealed that the peaks of in-cylinder pressure and heat release rate were higher when employing microwave ignition compared to conventional spark ignition. The study's additional findings indicate that whereas the COVimep of conventional spark ignition may approach 20 at λ=1.35, it maintained a value below 15 at λ=1.5 when microwave ejection was used (Fig. 6). This is because the advanced combustion phase increased the in-cylinder pressure, which in turn enhanced the microwave-assisted plasma ignition's IMEP [67-70]. According to these findings [39], the microwave-assisted plasma ignition as shown in Fig. 5, can reduce the fuel consumption i.e. 2.05% increase in fuel efficiency in this case and avoid the lean limit flame out of a cylinder.

4.2 Spark Discharge Current

5% was the COV limit in the research conducted by Jung et al. [48]. The definition of the lean limit was thus the leanest condition that did not exceed the COV limit. In the absence of a discharge gap, the COV of IMEP reached 8.0% at λ =2.1. Yet, even at λ=2.1, the COV was reduced to less than 5% at a discharge interval of 0.4ms. With the exception of the high CCV conditions, the thermal efficiency increased as the extra air ratio increased. This effect can be explained by the decrease in heat loss. It is also possible that CCV suppression contributed to the increase in thermal efficiency at a discharge interval (Δti) of 0.4ms. Although the COV of IMEP reached 6.70%, an operation at λ=2.3 was attained and the maximum indicated thermal efficiency of 47.9% was achieved when the discharge interval was 0.4ms. According to Jung et al. [48] additional research on multiple spark discharge using a multi-coil ignition system to improve the thermal efficiency of lean SI engine operation, the indicated thermal efficiency increases fairly linearly with increasing λ for all discharge intervals taken into consideration. Additionally, for all but the Δti = 0.3ms example, the longer Δti is shown to have a greater the indicated thermal efficiency at each λ. Moreover, the lower COV of IMEP can be obtained by the longer Δti. The maximum the indicated thermal efficiency (≈47.0%) was thus obtained for operation with the multiple spark discharge of Δti = 0.2ms at about λ = 1.94.

4.3 Injection Strategy

When comparing the variation in combustion stability with the excess air ratio at different injection pressures for a single or split injection strategy, Park et al. [25] discovered that employing split injection extends the flammability limit with a high excess air ratio (e.g., λ = 2.0), while maintaining a COV_{IMEP} value of 5% as a benchmark for stable combustion. The study investigated how a split-injection strategy impacts the performance of stratified lean combustion in a gasoline direct-injection engine. The effect of the excess air ratio further expanding on the combustion stability was also studied and as λ expanded further, the COV_{IMEP} value increased as shown in Fig. 6. Improved stratified mixture ignitability with a twofold injection method reduces fuel consumption rate and COV_{IMEP} (Fig 5 and Fig 6 respectively), according to additional research [71].

Astanei et al came at a similar conclusion [51]. Furthermore, as the obtained results show, a high injection pressure is required to accomplish stable stratified lean combustion [25, 72].

4.4 Fuel Blending and Pre-chamber addition

Jamrozik et al. conducted a comparison between test results from a conventional gasoline engine featuring a single-stage combustion system and a slightly higher compression ratio of 9, and results from tests carried out on a dual-fuel engine equipped with a two-stage combustion system. In the latter, gasoline powered the cylinder while LPG fueled the pre-chamber [26, 43, 73]. The value of IMEP decreased by 16.7% in the engine with a conventional combustion system, but it decreased by 23.6% in the dual-fuel engine (LPG + Gasoline Prechamber) with the extension of the excess air ratio brought about by the addition of the prechamber. In comparison to the traditional engine, the dual fuel engine's higher IMEP decline also suggests a higher in-cylinder temperature decrease, which results in a lower maximum indicated thermal efficiency. On the other hand, an engine with a conventional combustion system experienced an increase in indicated thermal efficiency up to 34.2%, while a gas engine with a two-stage combustion system saw its maximum Indicated Thermal Efficiency (ITE) at λ = 1.8 (Fig. 7). This increase was followed by an increase in the excess air ratio λ up to 2.3. The COV_{IMEP} as shown in Fig. 6 indicated that further blending of the mixture to a maximum value of λ = 1.5 was linked with greater non-repeatability of engine cycles and decreased the engine's ITE [43].

Other engine performance experiments revealed that using fuel combined with ethanol and gasoline will result in a slight increase in torque output at small throttle valve openings [55].

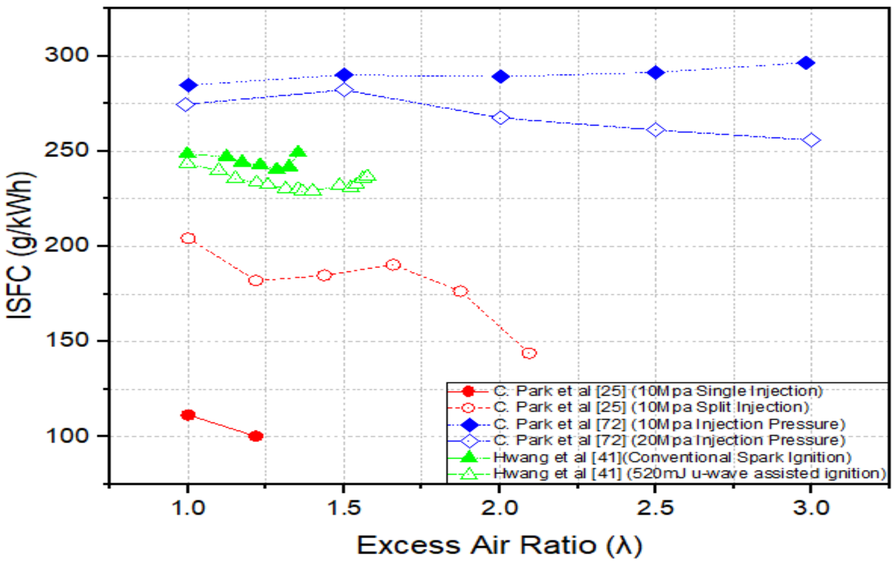

Fig. 5. The effect of excess air ratio on the specific fuel consumption

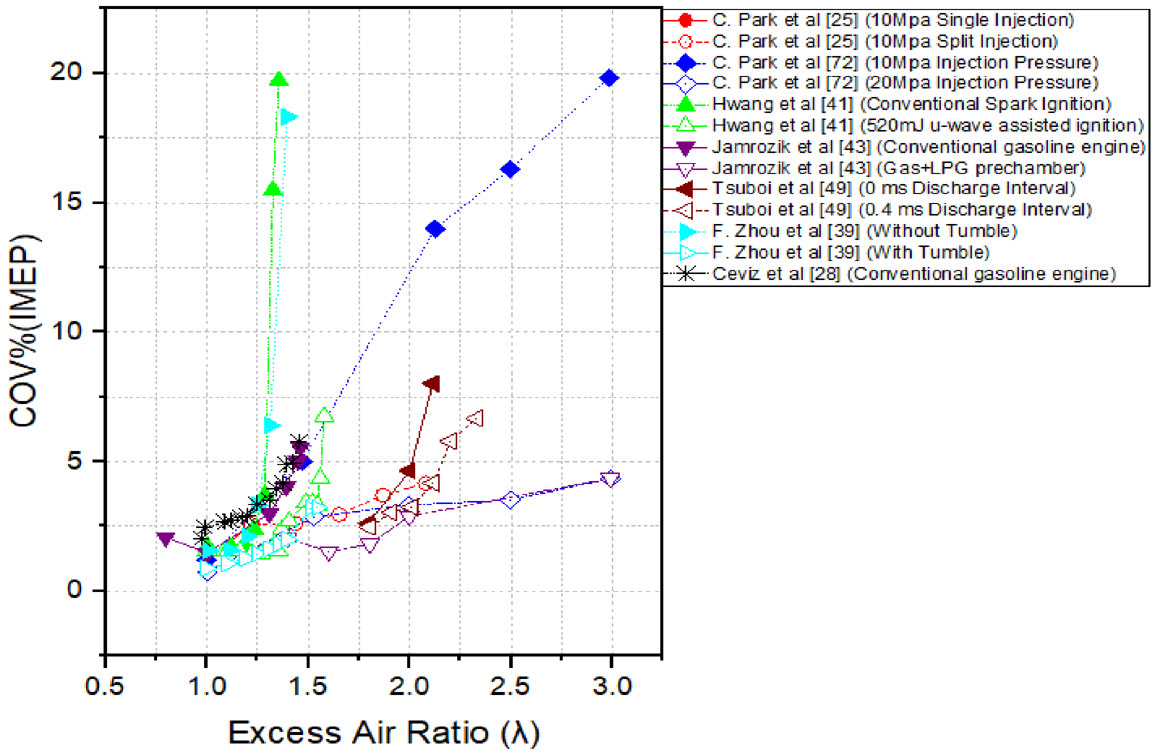

Fig. 6. The effect of excess air ratio on the coefficient of variation of indicated mean effective pressure

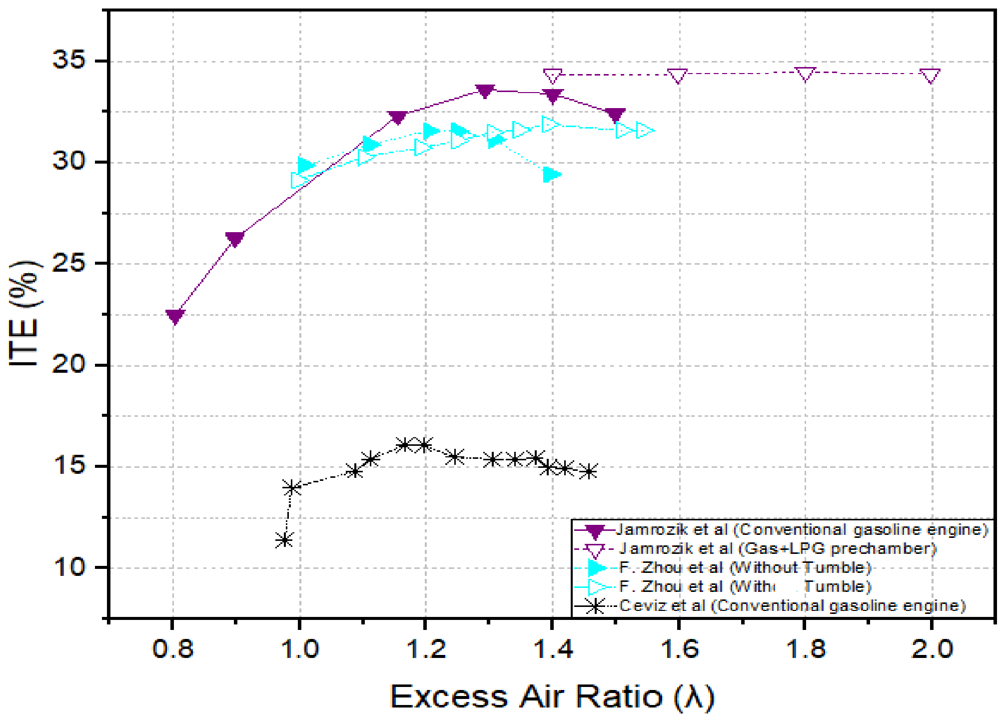

Fig. 7. The effect of excess air ratio on the engine indicated thermal efficiency

5. CONCLUSION

From the review, the importance of the air-fuel ratio in combustion has been discussed. In the case of excess air, its influence on emissions, engine performance and efficiency have been reviewed. Additionally, ultra-lean burn was considered as it seemingly showed to be a viable means to reduce Greenhouse Gases emissions. The effect of this combustion mode has on engine performance and efficiency is studied. The following are the conclusions from the review:

1. The air-fuel ratio is an important factor in combustion as it controls the amount of energy released, the amount of undesired pollutants generated during the process, and whether a mixture is combustible or not.

2. For lean burn, NOx emissions increase with improved combustion and better air/fuel mixing (λ=1.0 to 1.2). At this point, HC and CO emissions decrease. Further increasing the excess mass of air, the heat release and the average combustion temperature are reduced due to the more diluted mixture. This results in lower NOx emissions. However, in the case of HC and CO emissions, the incomplete combustion and combustion instability associated with high levels of excess air ratio causes a rise in these emissions.

3. The COV_{IMEP}, the value indicating combustion stability, since the indicated mean effective pressure decreases as the value of λ increases, resulting in a decline in performance utility caused by the depletion excess air ratio mixture, this value to increase. When the combustion stability is achieved, the Indicated Specific Fuel Consumption typically drops because there is less pumping loss as the extent of lean conditions rises. In the case of combustion instabilities, i.e. in higher excess air ratio values in conventional engines, the ISFC value increases.

4. The reduction in heat release under lean combustion results in the reduction in thermal efficiency. This showed that in this study there is a trade-off between efficiency and NOx emissions.

5. Given the specific range where fuel to air ratios must fall for ignition to occur, various methods, including adjustments to engine design, operational parameters, and improvement of fuels, can be employed to attain stable combustion. Achieving stable combustion, particularly in ultra-lean conditions, results in better efficiency, reduced fuel consumption, and lower emissions compared to a conventional spark ignition engine operating in lean combustion mode.

6. RECOMMENDATION

The different methods to achieve ultra-lean combustion outlined in this review can be improved. Especially in enhancing fuel properties by the use of fuel additives (ex. Nanofuels) or using different gasoline-biofuel blends. Hydrogen and Acetylene gas are also fuels that can be blended with gasoline to reduce emissions and also to investigate the performance of the engine under ultra-lean combustion.

REFERENCES

[1] Lauber J, Guerra TM, Dambrine M (2011) Air-fuel ratio control in a gasoline engine. Int J Syst Sci 42(2):277–286

[2] Poloni T, Johansen T, Rohal'-Ilkiv B (2006) Modeling of air-fuel ratio dynamics of gasoline combustion engine with ARX network,

[3] Ohata A, et al. Model-Based Air Fuel Ratio Control for Reducing Exhaust Gas Emissions, SAE Paper 950075, Detroit, U.S.A., 1995.

[4] Suzuki K, Shen T, et al. Individual A/F Control with Fuel-Gas Estimation for Multi-Cylinder IC Engines, IEEE paper 0018-9545, New York, U.S.A., 2009.

[5] Anderson M: A feedback A/F control system for low emission vehicles, SAE Paper, No. 930388, 1993.

[6] Yasui Y, Kawasumi I And Higashitani, K, A New Air-Fuel Ratio Control for a High-Efficiency and Low-Emission Engine, SICE Journal of Control, Measurement, and System Integration, Vol. 5, No. 5, pp. 268–275, September 2012

[7] Fekete P J et al., "Mode1-based air-fuel ratio control of a lean multicylinder engine.," SAE paper 950846,1995

[8] Liu Ya-bin, et al. Forecast of gas line status at real time based on modified Elman neural network [J]. Journal of Systems Engineering, 2003,18(5):475-478

[9] Tafreshi, R., Ebrahimi, B., Mohammadpour, J., Franchek, M.A., Grigoriadis, K. and Masudi, H., "Linear Dynamic Parameter-Varying Sliding Manifold for Air–Fuel Ratio Control in Lean-burn Engines", IET Control Theory & Applications, vol.7 issue 10, pp.1319-1329, 2013.

[10] Wang, P., Zhu, C. and Gao, J., "Feedforward Model Predictive Control of Fuel-Air Ratio for Lean-burn Spark-Ignition Gasoline Engines of Passenger Cars", IEEE Access, vol.7, 2019.

[11] Kumar, M. and Shen, T., "In-cylinder Pressure-based Air-Fuel Ratio Control for Lean Burn Operation Mode of SI Engines", Energy, vol.120, pp.106-116, 2017.

[12] Wu, H.M. and Tafreshi, R., "Fuzzy Sliding-mode Strategy for Air–Fuel Ratio Control of Lean-Burn Spark Ignition Engines", Asian Journal of Control, vol.20, issue 1, pp.149-158, 2018.

[13] Zope, R.A., Mohammadpour, J., Grigoriadis, K.M. and Franchek, M., "Air-fuel ratio control of spark ignition engines with TWC using LPV techniques", In Dynamic Systems and Control Conference, vol. 48920, pp. 897-903, 2009.

[14] Wu, H. M., & Tafreshi, R., "Air–fuel ratio control of lean-burn SI engines using the LPV-based fuzzy technique", IET Control Theory & Applications, vol.12, issue 10, pp.1414-1420, 2018

[15] Zhang, F., Grigoriadis, K. M., Franchek, M. A., and Makki, I. H. (January 25, 2007). "Linear Parameter-Varying Lean Burn Air-Fuel Ratio Control for a Spark

Ignition Engine." ASME. J. Dyn. Sys., Meas., Control. July 2007; 129(4): 404–414.

[16] Wang, L., Zhang, W. Y., & Pei, Y. Q. (2011). Fuzzy Auto-Tuning Techniques Applied to Air-Fuel Ratio Control on a Lean Burn Engine. In Applied Mechanics and Materials (Vol. 127, pp.434–438.Trans Tech Publications, Ltd. https://doi.org/10.4028/www.scientific.net/amm.127.434.

[17] Honek M, Gulan M, Vlad C, Rohal-Ilkiv B, Hybrid MPC for gasoline engine air-fuel ratio control using optimal PWA approximation, IFAC Papers Online 50-1 (2017) 2878–2885

[18] Lenz U, Schroeder, D, Transient air-fuel ratio control using artificial intelligence, SAE Paper (1997) 9706l8. DOI: 10.4271/970618

[19] Pielecha, I, Wislocki, K, Cieslik, W and Fiedkiewicz, L, Prechamber selection for a two-stage turbulent jet ignition of lean air-gas mixtures for better economy and emission, E3S Web Conf., 70 (2018) 03010, DOI: https://doi.org/10.1051/e3sconf/20187003010

[20] Ahmad O. Hasan, Ahmad Abu-Jrai, Ala'a H. Al-Muhtaseb, Athanasios Tsolakis, Hongming Xu, HC, CO and NOx emissions reduction efficiency of a prototype catalyst in gasoline bi-mode SI/HCCI engine, Journal of Environmental Chemical Engineering, Volume 4, Issue 2, 2016, Pages 2410-2416, ISSN 2213-3437, https://doi.org/10.1016/j.jece.2016.04.015.

[21] Dec, J. E.; Sjöberg, M. A parametric study of HCCI combustion the sources of emissions at low loads and the effects of GDI fuel injection. SAE [Tech. Pap.] 2003, No. 2003-01-0752

[22] Nitrogen Oxides (NOx), Why and How They Are Controlled Prepared by Clean Air Technology Center (MD-12) Information Transfer and Program Integration Division Office of Air Quality Planning and Standards U.S. Environmental Protection Agency Research Triangle Park, North Carolina 27711. https://www3.epa.gov/ttncatc1/dir1/fnoxdoc.pdf

[23] Li, G, Long, Y, Zhang, Z, Liang, J, Zhang, X, Zhang, X, Wang, Z, Performance and emissions characteristics of a lean-burn marine natural gas engine with the addition of hydrogen-rich reformate, International Journal of Hydrogen Energy, Volume 44, Issue 59, 2019, Pages 31544-31556, ISSN 0360-3199, https://doi.org/10.1016/j.ijhydene.2019.10.007.

[24] Ivanič Ž, Ayala F, Goldwitz J and Heywood J B, Effects of Hydrogen Enhancement on Efficiency and NOx Emissions of Lean and EGR-Diluted Mixtures in a SI Engine 2005 SAE Paper 2005-01-0253

[25] Park C, Kim S, Kim H, Lee S, Kim C, Moriyoshi Y. Effect of a split-injection strategy on the performance of stratified lean combustion for a gasoline direct-injection engine. Proceedings of the Institution of Mechanical Engineers, Part D: Journal of Automobile Engineering. 2011;225(10):1415-1426. doi:10.1177/0954407011406469

[26] Jamrozik, Arkadiusz & Tutak, Wojciech. (2011). A study of performance and emissions of SI engine with a two-stage combustion system. CHEMICAL AND PROCESS ENGINEERING. 32. 453-471. 10.2478/v10176-011-0036-0.

[27] Arcoumanis, C., Gold, M.R., Whitelaw, J.H., & Xu, H.M. (1999). Local mixture injection to extend the lean limit of spark-ignition engines. Experiments in Fluids, 26, 126-135

[28] Ceviz, Mehmet & Oner, Volkan & Kaya, Ferhat & Karacali, Tevhit. (2011). Analysis of the thermal efficiency and cyclic variations in a si engine under lean combustion conditions. Isi Bilimi Ve Teknigi Dergisi/ Journal of Thermal Science and Technology. 31. 121-127.

[29] Park C, Lee S, Yi U, Effects of engine operating conditions on particle emissions of lean-burn gasoline direct-injection engine, Energy, Volume 115, Part 1, 2016, Pages 1148-1155, ISSN 0360-5442, https://doi.org/10.1016/j.energy.2016.09.051.

[30] Martinez S, Irimescu A, Merola SS, Lacava P, Curto-Riso P. Flame Front Propagation in an Optical GDI Engine under Stoichiometric and Lean Burn Conditions. Energies. 2017; 10(9):1337. https://doi.org/10.3390/en10091337

[31] Kumar M, Shen T, In-cylinder pressure-based air-fuel ratio control for lean burn operation mode of SI engines, Energy, Volume 120, 2017, Pages 106-116, ISSN 0360-5442, https://doi.org/10.1016/j.energy. 2016.12.091.

[32] Heywood, John B. 2018. Internal Combustion Engine Fundamentals. 2nd ed. New York: McGraw-Hill Education.

[33] Boretti A.A, Watson H.C, The lean burn direct injection jet ignition gas engine, International Journal of Hydrogen Energy, Volume 34, Issue 18, 2009, Pages 7835-7841, ISSN 0360-3199, https://doi.org/10.1016/j.ijhydene.2009.07.022.

[34] Huang, Shuai & Li, Tie & Ma, Pengfei & Xie, Siyu & Zhang, Zhifei & Chen, Run. (2019). Quantitative Evaluation of the Breakdown Process of Spark Discharge for Spark-Ignition Engines. Journal of Physics D : Applied Physics. 53. 10.1088/1361-6463/ab56da.

[35] Yu X, Yang Z, Yu S, Huo X, Ting D, Zheng M and Li L 2018 SAE Paper 2018-01-1133

[36] https://inventions.prf.org/innovation.html?InventionID=6175

[37] Li Y, Zhao H, Ma T, Stratification of fuel for better engine performance, Fuel, Volume 85, Issue 4, 2006, Pages 465-473, ISSN 0016-2361, https://doi.org/10.1016/j.fuel.2005.08.005.

[38] Park C, Kim S, Kim H and Moriyoshi Y, (2012), Stratified lean combustion characteristics of a spray-guided combustion system in a gasoline direct injection engine, Energy, 41, (1), 401-407

[39] Zhou F, Fu J, Ke W, Liu J, Yuan Z, Luo B, Effects of lean combustion coupling with intake tumble on economy

and emission performance of gasoline engine, Energy, Volume 133, 2017, Pages 366-379, ISSN 0360-5442, https://doi.org/10.1016/j.energy.2017.05.131.

[40] Wang Z, Li X, Gao X, Chen D, Zhu Z. Experimental Research on the Influence of Microwave Radiation on Coal Permeability and Microstructure. ACS Omega. 2021 Dec 7;6(50):34375-34385. doi: 10.1021/acsomega.1c04291. PMID: 34963923; PMCID: PMC8697008.

[41] Hwang, Joonsik & Kim, Wooyeong & Bae, Choongsik & Choe, Wonho & Cha, Jeonghwa & Woo, Soohyung, 2017. "Application of a novel microwave-assisted plasma ignition system in a direct injection gasoline engine," Applied Energy, Elsevier, vol. 205(C), pages 562-576.

[42] Serrano D, Zaccardi J-M, Müller C, Libert C, Habermann K, Ultra-Lean Pre-Chamber Gasoline Engine for Future Hybrid Powertrains, 14th International Conference on Engines & Vehicles, Sep 2019, Capri, Italy.

[43] Jamrozik, A. Lean combustion by a pre-chamber charge stratification in a stationary spark ignited engine. J Mech Sci Techno 29, 2269–2278 (2015). https://doi.org/10.1007/s12206-015-0145-7

[44] Oliveira C, Reis J L Jr, Souza-Corrêa J A, Dal Pino A Jr and Amorim J, Optical and electrical diagnostics of a spark-plug discharge in air, 2012 J. Phys. D: Appl. Phys. 45 1–7

[45] Maly R, Spark ignition: its physics and effect on the internal combustion engine, 1984 (Berlin: Springer) pp 91–148

[46] Kawahara N, Hashimoto S, Tomita E, Spark discharge ignition process in a spark-ignition engine using a time series of spectra measurements, Proceedings of the Combustion Institute, Volume 36, Issue 3, 2017, Pages 3451-3458, ISSN 1540-7489, https://doi.org/10.1016/j.proci.2016.08.029.

[47] Stone R, Introduction to Internal Combustion Engines (3rd ed.), Society of Automotive Engineers, Inc., Warrendale (1999)

[48] Jung, Dongwon & Iida, Norimasa, 2018. "An investigation of multiple spark discharge using multi-coil ignition system for improving thermal efficiency of lean SI engine operation," Applied Energy, Elsevier, vol. 212(C), pages 322-332, DOI: 10.1016/j.apenergy.2017.12.032

[49] Tsuboi S, Miyokawa S, Matsuda M, Yokomori T, Iida N, Influence of spark discharge characteristics on ignition and combustion process and the lean operation limit in a spark ignition engine, Applied Energy, Volume 250, 2019, Pages 617-632, ISSN 0306-2619, https://doi.org/10.1016/j.apenergy.2019.05.036.

[50] Nakata, K., Nogawa, S., Takahashi, D., Yoshihara, Y., Kumagai, A., & Suzuki, T. (2016). Engine Technologies for Achieving 45% Thermal Efficiency of S.I. Engine. SAE International Journal of Engines, 9(1), 179–192. http://www.jstor.org/stable/26284804

[51] Astanei, D., Faubert, F., Pellerin, S. et al. Evaluation of the Efficiency of a Double Spark Plug to Improve the Performances of Combustion Engines: Pressure Measurement and Plasma Investigations. Plasma Chem Plasma Process 40, 283–308 (2020). https://doi.org/10.1007/s11090-019-10044-3

[52] Boston, P.M., Dradlry, D. Et al., “Flame Initiation in Lean, Quiescent and Turbulent Mixtures with Various Igniters”, Twentieth Symposium (International) on Combustion, the Combustion Institute, pp.141-149, 1984

[53] Swords, M.D., Alghatgi, G.T., and Watts, A.J., “An experimental Study of Ignition and Flame Development in a Spark Ignited Engine”, SAE Paper 821220, 1982

[54] Pundir, B. P., Emission Reduction in Small SI Engine Generator Sets, SAE 2004-011089 (2004).

[55] Wu C-W, Chenb R-H, Pua J-Y, Lina T-H, the influence of air–fuel ratio on engine performance and pollutant emission of an SI engine using ethanol–gasoline-blended fuels, Atmospheric Environment 38 (2004) 7093–7100.

[56] Li T, Yin T and Wang B, Anatomy of the cooled EGR effects on soot emission reduction in boosted spark-ignited direct-injection engines, 2017 Appl. Energy 190 43–56

[57] Li T, Wu D and Xu M, Thermodynamic analysis of EGR effects on the first and second law efficiencies of a boosted spark-ignited direct-injection gasoline engine, 2013 Energy Convers. Manage. 70 130–8

[58] Minh K. Le, Atsushi Nishiyama, Takeshi Serizawa, Yuji Ikeda, Applications of a multi-point Microwave Discharge Igniter in a multi-cylinder gasoline engine, Proceedings of the Combustion Institute, Volume 37, Issue 4, 2019, Pages 5621-5628, ISSN 1540-7489, https://doi.org/10.1016/j.proci.2018.06.033.

[59] Starikovskiy, A.; Aleksandrov, N. Plasma-assisted ignition and combustion. Prog. Energy Combust. Sci. 2013, 39, 61–110.

[60] Ju, Y.G.; Sun, W.T. Plasma assisted combustion: Dynamics and chemistry. Prog. Energy Combust. Sci. 2015, 48, 21–83. Sensors 2023, 23, 5056 18 of 19

[61] Popov, N.A. Kinetics of plasma-assisted combustion: Effect of non-equilibrium excitation on the ignition and oxidation of combustible mixtures. Plasma Sources Sci. Technol. 2016, 25, 043002.

[62] Popov, N.A.; Starikovskaia, S.M. Relaxation of electronic excitation in nitrogen/oxygen and fuel/air mixtures: Fast gas heating in plasma-assisted ignition and flame stabilization. Prog. Energy Combust. Sci. 2022, 91, 100928.

[63] He, L.M.; Liu, X.J.; Zhao, B.B.; Jin, T.; Yu, J.L.; Zeng, H. Current investigation progress of plasma-assisted ignition and combustion. J. Aerospace. Power 2016, 31, 1537–1551.

[64] Fu, W. Research on Matching Characteristics of Plasma Assisted CH4 Combustion. Master’s Thesis, Harbin Institute of Technology, Harbin, China, 2020

[65] Pertl F., Smith J. Electromagnetic design of a novel microwave internal combustion engine ignition source, the quarter wave coaxal cavity igniter. Proc. IMechE, Part D: J. Automobile Engineering, 2009, 223(11), 1405–1417.

[66] Hirsch, N.; Gallatz, A. Space ignition method using microwave radiation. MTZ Worldwide 2009, 70, 32–35.

[67] Zhang, G.X.; Hou, L.Y.; Wang, Q.; Liu, Y.X.; Huang, J.; Wang, Z. Method to realize multi-point ignition based on the microwave resonant of transverse magnetic resonant mode (TM010). J. Automotive. Energy 2015, 6, 179–183.

[68] Liu, C.; Zhang, G.X.; Xie, H.; Deng, L.; Wang, Z. Exploring microwave resonant multi-point ignition using high-speed schlieren imaging. Rev. Sci. Instrumentation. 2018, 89, 034701.

[69] Liu, C.; Zhang, G.X.; Xie, H.; Deng, L. Experimental Development of microwave l study of multipoint ignition in methane–air mixtures by pulsed microwave power. IEEE Trans. Plasma. Sci. 2018, 46, 3499–3503

[70] Liu, C.; Zhang, G.X.; Xie, H.; Deng, L.; Wang, Z. Experiment investigation of multi-point microwave ignition by high-speed schlieren method. J. Eng. Thermophysics. 2018, 39, 662–665

[71] Park, C.W., Oh, H.C., Kim, S.D. et al. Evaluation and visualization of stratified ultra-lean combustion characteristics in a spray-guided type gasoline direct-injection engine. Int.J Automotive. Technol. 15, 525–533 (2014). https://doi.org/10.1007/s12239-014-0055-1

[72] Park C; Kim S; Hongsuk Kim H and Moriyoshi Y, (2012), Stratified lean combustion characteristics of a spray-guided combustion system in a gasoline direct injection engine, Energy, 41, (1), 401-407

[73] Cupiał, K., Jamrozik, A., & Spyra, A. (2002). Single and two–stage combustion system in the SI test engine. Journal of KONES, 67-74

Energy, Environment and Storage

Journal Homepage: www.enenstrg.com

Experimental Investigation of Energy Analysis of Methanol-Gasoline Mixtures at Different Torque Values

Ahmet Turan Dumanli[1], Bilge Albayrak Çeper[2], Talip Akbiyik[3], Nafiz Kahraman[2]

[1] Dept. Of Mechanical Engineering, Erciyes University

[2] Dept of Aerospace Engineering, Erciyes University

[3] Department of Motor Vehicles and Transportation Technology, Aksaray University, Aksaray

I. **ABSTRACT**. Despite the increasing use of petroleum-based fuel as a result of ever-increasing energy demands, the search for alternative fuels remains important. In this study, in a Lombardini LGW 523 brand 2-cylinder 4-stroke water-cooled engine, different volumetric ratios of methanol and gasoline fuel mixtures (M10, M20, M30, M40) were used at 4 different torque values (5, 10, 15, 20 Nm) at a constant 3000 engine speed. It is discussed. As a result of the study, engine performance, emission and energy analysis examination was carried out experimentally.

.

Keywords: Energy, Exergy, Internal Combustion Engine, Methanol Fuel

Article History: Received: 04.04.2024; Accepted: 24.05.2024; Available online: 31.05.2024
Doi: https://doi.org/10.52924/SAOW6955

1. INTRODUCTION

Unlike fossil fuels, biomass is a renewable alternative energy source because vegetation renews itself every year. Therefore, biomass energy is important as a sustainable energy source. Additionally, while resources such as wood, biomass and biogas are considered non-commercial fuels, for example leaves, corn cobs, pea pods, algae, bacteria, algae and any form of fertilizer are fuels with commercialization potential [1].

Biodiesel, which is an alternative fuel obtained through biomass technology, can be produced from used or unused vegetable and animal oils by various methods. Since biodiesel fuel properties are very similar to those of diesel, it can be used alone or mixed with diesel fuel in different proportions in diesel engines without any problems [2]. Atabani et al.[3], detailed the raw material source of biodiesel, its extraction, biodiesel production methods, properties and quality of biodiesel, problems and potential solutions of using vegetable oil in biodiesel production, advantages and disadvantages of biodiesel, its economic feasibility and sustainability, and its future. They were examined in this way. Suresh et al. [4], in their study, examined the effects of biodiesel obtained from waste cottonseed oil on engine performance and exhaust emissions. According to the test results, they revealed that biodiesel reduces thermal efficiency, low biodiesel ratio reduces specific fuel consumption, increases NO emissions while reducing CO and HC emissions. However, they stated that the addition of biodiesel to diesel fuel increased the maximum cylinder pressure values. Yang et al.[5], examined the use of biodiesel obtained from waste cooking oil directly in a diesel engine and engine performance and emission analysis. As a result, they revealed that biodiesel reduced engine torque and power values and increased specific fuel consumption values. Özsezen and Çanakçı [6], mixed the biodiesel obtained from waste palm oil into diesel fuel at a ratio of 5-20-50% and compared the engine performance and emission parameters according to biodiesel and diesel fuel. They found that there was a decrease in engine torque and an increase in specific fuel consumption associated with the increasing percentage of biodiesel in the mixture. Ref [7] determined the engine performance and exhaust emission values using gasoline, pentanol-gasoline, hexanol-gasoline, and heptanol-gasoline in a spark-ignition engine (SIE) at a different load conditions and under constant speed. They analyzed a lot of parameters (energy, exergy, economic, environmental, and sustainability). Their results concluded that the addition of different heavy alcohols to gasoline, reduces the thermal efficiency and increases the fuel consumption.

Sayin Kul and Ciniviz [8], investigated energy and exergy analyses by blending two different bioethanol with

*Corresponding author: balbayrak@erciyes.edu.tr

gasoline on an SI engine. They prepared their fuels by adding both bioethanol, one of them was produced from waste bread and the other from sugar beet. They carried out the tests at 5 different engine loads and 2500 rpm. As a result of the study, the addition of bioethanol had a reducing effect on the rates of energy loss, exergy destruction and exergy loss.

Doğan et al [9], experimentally investigated effects of fuel blends in different proportions on exhaust emissions and engine performance. Experiments have been carried out at different engine speeds (1250–3000 rpm) and different blends (D100, F5, F10, F20, F30, and F37) in the full load conditions. In their studies, they also conducted exergy, energy, and exorgoeconomic analyses. They observed that the addition of fusel oil to diesel demostrated a significant decrease in NOX, CO2 emissions and a significant increase in particulate matter, CO and HC emissions.

Using safflower (Carthamus tinctorius L.) oil methyl ester (SOME) and conventional diesel at varying engine loads and constant engine speed (1500 rpm), Yaman [10] examined the energy and exergy analyses. Their findings demonstrate that as load and CR increased so did the energetic and exegetic efficiency values. In an internal combustion engine operating at less than 100 Nm, biodiesel and diesel fuels were experimentally examined by Yıldız et al. [11]. Energy, energy consumption, and environmental effects were examined with and without an after treatment system using a silicon carbide-based diesel particle filter (SiC-DPF). When SiC-DPF is used, CO2 emissions from biodiesel fuel are reduced, while those from diesel fuel are increased. The methanol/biodiesel blends were studied by Xu, G. et al. [12] under various engine loads, speeds, and conditions. Several structural factors, including average particle size, specific surface area, average pore radius, and pore volume of particulate matter, were taken into account in their investigations. The effects of methanol additives and Jatropha biodiesel-diesel blends on a single-cylinder diesel engine were obtained by Rai, R. V. et al. [13]. They observed that engine power, effective efficiency, volumetric efficiency, and specific fuel consumption value were all increased when biodiesel-methanol blend fuels were used.

As can be seen when the literature is examined, there are many studies on energy and exergy analyzes of biomass-fueled thermal power plants, and recently, studies on energy and exergy analyzes in internal combustion engines have increased. This study contributed to the literature by presenting energy analysis for methanol added to gasoline at different torque values.

2. MATERIALS AND METHODS

2.1 The Experimental Setup

The experimental setup consists of engine, eddy current dynamometer, measurements system, emission device, and fuels (gasoline and methanol). The experiments were carried out in Dept. of Mechanical engineering engine laboratory in Erciyes University. The experimental setup system is given in Fig. 1.

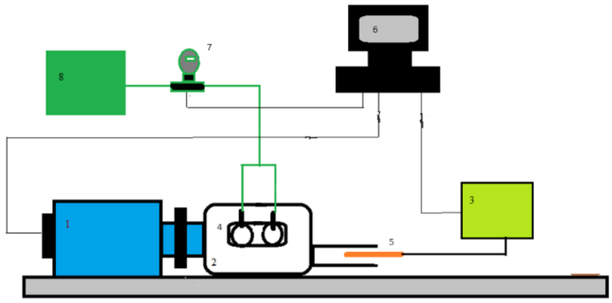

Fig. 1. Schematic view of the experimental setup

1 dynamometer, 2 engine, 3 exhaust emission device, 4 petrol injectors, 5 exhaust probe, 6 computer, 7 liquid flow meter, 8 fuel tank,

A 2-cylinder, 4-stroke spark ignition Lombardini LGW 523 MPI engine, whose specifications are given in Table 1, was used in the experiments. In the experiments, 90% gasoline - 10% methanol (M10), 80% gasoline - 20% methanol (M20), 70% gasoline - 30% methanol (M30) and 60% gasoline - 40% methanol (M40) mixtures were used at 3000 rpm. It was tested at 4 different torque values (5, 10, 15 and 20 Nm) at constant engine speed.

Table 1. Lombardini LGW 523 engine features [14]

Engine Type	Unit	Value
Number of cylinders	-	2
Diameter of the cylinder	mm	72
Stroke	mm	62
Cylinder volume	cc	505
Stroke ratio	-	10, 7:1
Revolution maximum	rpm	5500
Max. of the power (5000 rpm)	kW/HP	15/20.4
Max. of the torque (2150 rpm)	Nm	34

SAJ brand SE150 model eddy current electric dynamometer was used for torque and power measurements. Gasoline and Methanol flow rates were determined with a liquid mass Krohne Optimass 3300C brand device. Exhaust gas measurements were carried out with a Bosch BEA 060 gas analyzer, and the features and error ranges of the equipment and sensors are given in Table 2.

Table 2. Specifications and error ranges

Instrument	Values	Accuracies
Liquid flow meter	1.2–130 kg/h	±0.035%
Hot film air mass meter (Bosch HFM 5)	10–480 kg/h	≤3%
Eddy Current Dynamometer	150 kW/8000 rpm	±1 rpm
Exhaust gas analyzer (Bosch BEA 060)		
CO	0–10% Vol	0.001% vol
CO_2	0–18% Vol	0.010% vol
O_2	0–22% Vol	0.010% vol
NO_x	0–5000 ppm	1.0 ppm
HC	0–9999 ppm	1.0 ppm
Lambda	0.5–9.999	0.001

Before the experiments, the test engine was run at idle until it reached the regime temperature. After the engine reached the regime temperature, the load was gradually increased with the Eddy Current dynamometer until the maximum load value, and the tests were repeated at different torque values by applying load to the engine.

2.2 Thermodynamic Analyses

First law analysis of thermodynamics was discussed to determine the energy inputs and outputs in the system. Exergy analyzes are calculated with combustion products obtained from combustion reaction equations. For this reason, calculations were made for combustion according to the combustion reaction equation 1 given in the literature [15]. The complete combustion equation is also shown in equation 2.

$$a(C_{X1}H_{Y1}) + b(C_{X2}H_{Y2}O_{Z2}) + c(C_{X3}H_{Y3}) + d(O_2+3{,}76N_2) \rightarrow e(CO_2) + f(CO) + g(O_2) + h(H_2O) + i(N_2) \quad (1)$$

$$a(C_{X1}H_{Y1}) + b(C_{X2}H_{Y2}O_{Z2}) + c(C_{X3}H_{Y3}) + d(O_2+3{,}76N_2) \rightarrow e(CO_2) + f(H_2O) + g(N_2) \quad (2)$$

The following assumptions were made for energy and exergy analyses.

- The engine operates in steady state,
- The combustion air is assumed an ideal gas,
- There is no water vapor in the combustion air,
- Potential and kinetic energy effects are neglected.

2.3 Energy Analyses

As predicted by the first law of thermodynamics, the energy balance equation for the current engine system is shown by equation 3-5.

$$\sum \dot{E}_{in} = \sum \dot{E}_{out} \quad (3)$$

$$\dot{E}_{in} = \dot{E}_{fuel} \quad (4)$$

$$\dot{E}_{out} = \dot{E}_{W} + \dot{E}_{ex} + \dot{E}_{loss} \quad (5)$$

$\dot{E}_{in}$ total entering energy, $\dot{E}_{out}$ total outgoing energy,

$\dot{E}_{fuel}$ total chemical energy of the fuel entering the system

$\dot{E}_{W}$ net power produced, $\dot{E}_{ex}$ energy of the exhaust gases, $\dot{E}_{loss}$ the energy losses occurring in the system. $\dot{E}_{fuel}$, $\dot{E}_{W}$, $\dot{E}_{ex}$ and $\dot{E}_{loss}$ were calculated according to equations 6, 7, 8, 9 and 10, respectively.

$$\dot{E}_{fuel} = \dot{m}_{fuel}\, H_U \quad (6)$$

$$\dot{E}_{W} = \frac{2.\pi.M.n}{60\,.1000} \quad (7)$$

$$\dot{m}_{ex} = (\dot{m}_{fuel} + \dot{m}_{air})\, 0{,}98 \quad (8)$$

$$\dot{E}_{ex} = \dot{m}_{i}\varepsilon_{t} \quad (9)$$

$$\dot{E}_{loss} = \dot{E}_{fuel} - \dot{E}_{ex} - \dot{E}_{W} \quad (10)$$

Thermal efficiency of the system:

$$\eta = \frac{\dot{E}_{W}}{\dot{E}_{fuel}} \quad (11)$$

3. RESULTS AND DISCUSSION

3.1 Fuel consumption

M10 fuel was prepared by mixing the gasoline and methanol fuel used in the experiments volumetrically (90% gasoline + 10% methanol). Since methanol fuel has a lower calorific value, more fuel must be used to give the same torque values at the same speed. When fuel consumption is examined, as the amount of methanol increases, the hourly fuel amount increases. Figure 2 shows the variation of specific fuel consumption with Torque values. As torque values increased, specific fuel consumption values decreased. The reduction rate between 5 and 20 Nm torque values is 57.6% for M10 fuel, 52.8% for M20 fuel, 52.4% for M30 fuel and 51.1% for M40 fuel.

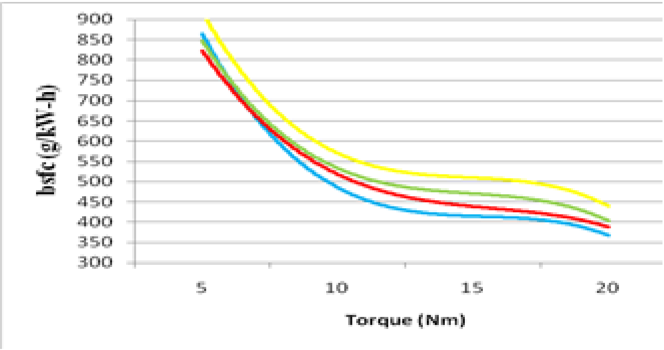

Fig. 2. Torque values versus the brake specific fuel consumption.

Figures 3 shows the changes in CO, CO2, HC, and NOx emissions depending on the torque value, respectively. When CO emissions were examined, it was observed that as the amount of methanol in the fuel increased, the amount of CO emissions decreased. The best results in CO2 emissions were obtained with M40 fuel. When HC emissions are examined, the amount of HC emissions is at a minimum level in the experiments conducted with M30 fuel. The calorific value of M10 blend fuel is the highest compared to other fuel blends, so the in-cylinder temperature is high. NOx emissions increased because the in-cylinder temperature was high. The high in-cylinder temperature also increased the exhaust gas energy and did not adversely affect combustion, on the contrary, it worsened the thermal efficiency. For this reason, it has been observed that HC emissions also increased. Regarding NOx emissions, it was observed that the highest NOx value was obtained in M10 fuel, as the calorific value of the fuel decreases as the amount of methanol in the fuel increases. In addition to increasing the amount of methanol in the mixture, the in-cylinder combustion temperature will decrease due to the low calorific value of methanol. For this reason, it is normal that the highest NOx emissions are in M10 fuel.

Energy distributions at different torque values are presented in Figures 4. As can be seen from this graph, as the torque value increased, the fuel energy values also increased. The formation of high combustion temperature with the increase in applied load increased the oxidation reaction of the products entering the combustion chamber. Additionally, higher temperature results in higher useful energy. As the torque value increases, the energy lost increase due to engine cooling water and exhaust gases, heat transfer and friction increases. It can be said that the reason for this increase is due to the increase in combustion temperature. As the torque increases, the rate of lost energy decreases. The best results in terms of fuel energy were obtained with M10 fuel. In terms of exhaust losses and lost energy, M30 fuel gave better results.

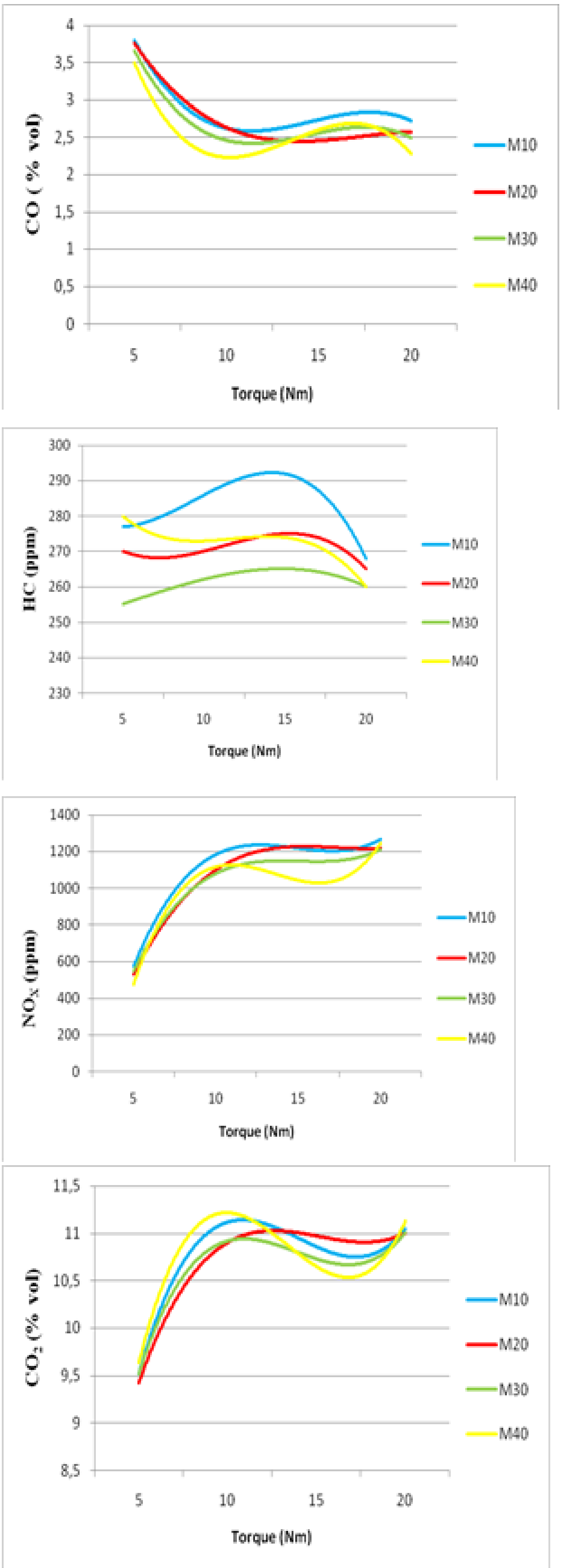

Fig. 3. Emission changes versus the torque values

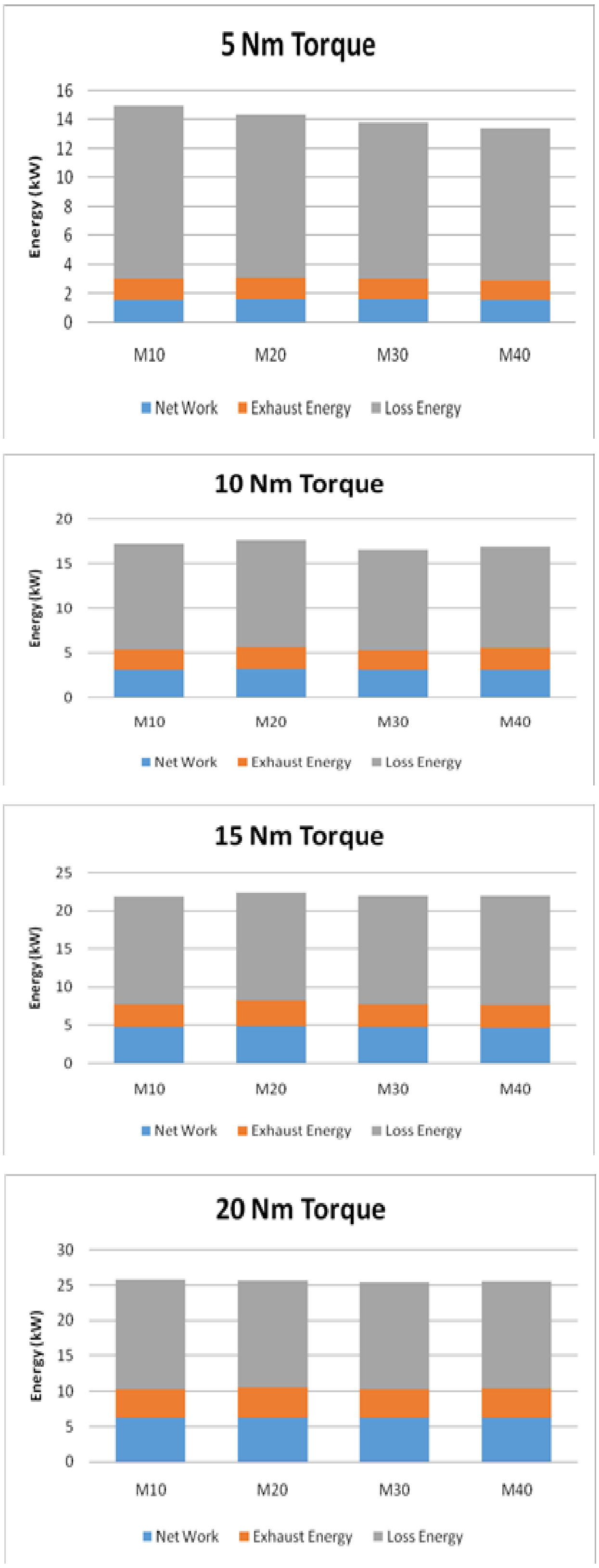

Fig 4. Energy changes at different torque values of different fuel mixtures

4. CONCLUSION

In this study, experimental examination of different volumetric ratios of methanol and gasoline fuel mixtures (M10, M20, M30, M40) at constant engine speed (3000 rpm) and 4 different torque values (5, 10, 15, 20 Nm) was carried out. The results obtained are briefly:

- When the torque values increase, the specific fuel consumption values decrease.
- Methanol added to the fuel resulted in a decrease in CO emissions. The best outcome in terms of CO2 emissions was achieved when using M40 fuel. When examining HC emissions, it was observed that the minimum level of HC emissions occurred in the experiments conducted with M30 fuel. In terms of NOx emissions, it was found that the highest NOx value was observed in the experiments conducted with M10 fuel.
- It was noticed that the fuel energy values increased with an increase in torque.
- When the torque increases, the rate of energy loss decreases.
- The M10 fuel produced the best fuel energy results, while M30 fuel had better results in terms of exhaust losses and lost energy.

Nomenclature

CI Compression Ignition

CO Carbon Monoxide

CR Compression Ratio

HC Hydrocarbon

HEP25 25% 1-heptanol + 75% gasoline

HEX25 25% 1-hexanol + 75% gasoline

NO Nitrous oxide

PEN25 25% 1-pentanol + 75% gasoline

SiC-DPF silicon carbide-based diesel particle filter

SOME Safflower oil methyl ester

REFERENCES

[1] Mesarovic, M., 2001. Sustainable energy from biomass, *Thermal Science*, 5 (2): 5-32.

[2] Kahraman, A., Ciniviz, M., Ors, I., Oguz, H., 2016. The Effect on Performance and Exhaust Emissions of Adding Cotton Oil Methyl Ester to Diesel Fuel, *Int J of Automotive Engineering and Technologies*, 5 (4): 148-154.

[3] Atabani, A.E., Silitonga, A.S., Badruddin, I.A., Mahlia, T.M.I., Masjuki, H.H., Mekhilef, S., 2012. A comprehensive review on biodiesel as an alternative energy resource and its characteristics, *Renewable and Sustainable Energy Reviews*, 16 (4): 2070-2093.

[4] Suresh, S., Sinha, D.,Murugavelh, S., 2016. Biodiesel production from waste cotton seed oil: engine performance and emission characteristics, *Biofuels*, 7 (6): 689- 698.

[5] Yang, H., Li, X., Mu, M., Kou, G.,Li, L., 2016. Performance and emissions analysis of a diesel engine directly fuelled with waste cooking oil biodiesel, *International Journal of Ambient Energy*, 38 (4): 428-434.

[6] Özsezen, A.N., Çanakçı, M., 2009. Analysis of Performance and Emissions in a Diesel Engine Fueled with

Biodiesel and Blends. Pamukkale University dept. of Engineering Fac. *Journal of Engineering Sciences*, 15 (2): 173-180

[7] Demirbas, M.,& Yesilyurt, M. K. (2023). Investigation of the behaviors of higher alcohols in a spark-ignition engine as an oxygenated fuel additive in energy, exergy, economic, and environmental terms. *Journal of Thermal Analysis and Calorimetry*, *148*(10), 4427-4462.

[8] Sayın Kul B, Ciniviz M. An evaluation based on energy and exergy analyses in SI engine fueled with waste bread bioethanol gasoline blends. *Fuel*. 2021;286:119375.

[9] Doğan B, Özer S, Erol D. Exergy, exergoeconomic, and exergoenviroeconomic evaluations of the use of diesel/fusel oil blends in compression ignition engines. *Sustain Energy Technol Assess*. 2022;53:102475.

[10] Yaman H. Investigation of the effect of compression ratio on the energetic and exergetic performance of a CI engine operating with safflower oil methyl ester. *Process Saf Environ Prot*. 2022;158:607–24.

[11] Yildiz I, Caliskan H, Mori K. Energy, exergy and environmental assessments of biodiesel and diesel fuels for an internal combustion engine using silicon carbide particulate filter. *J Therm Anal Calorim*. 2021;145(3):739–50.

[12] Xu G., Liu S., Jia H., Zhao Y., Zhang Q., Experimental investigation on the structure characteristics of methanol/biodiesel particulate matter, Fuel 332

[13] Rai V.R., Shringi D., Mathur Y.B., Performance evaluation of diesel-jatropha biodiesel-methanol blends in CI engine in, Mater. Today: Proc. Elsevier Ltd (2022)1561–1567

[14] Akbiyik, T., Kahraman, N., Taner, T., Investigation of the effect of boron additive to lubricating oil on engine performance, exhaust, and emissions, *Fuel*, Volume 312, 15 March 2022.

[15] Hoseinpour, M., Sadrnia, H., Tabasizadeh, M.,Ghobadian, B., 2017. Energy and exergy analyses of a diesel engine fueled with diesel, biodiesel-diesel blend and gasoline fumigation, *Energy*, 141: 2408-2420

Energy, Environment and Storage

Journal Homepage: www.enenstrg.com

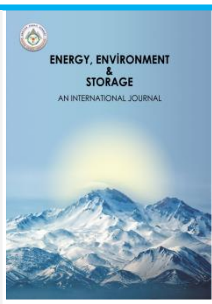

Aircraft Designed for Cargo Transportation and Investigation of its Benefits

Enes Özen[1*], Tuğrul Oktay[2]

[1*] *Hasan Kalyoncu University, Faculty of Engineering , Mechanical Engineering Department, Gaziantep, Turkey*

[2] *Erciyes University, Faculty of Aeronautics and Astronautics , Aeronautical Engineering Department, Kayseri, Turkey*

ABSTRACT. In this study, an Octorotor UAV capable of carrying 10 desi/2 kg cargo was designed. It is an eight-rotor rotary wing aircraft and its body consists of eight arms connected to each other by two moving mechanisms. When requested in emergency situations, the fastest intervention can be provided by aircrafts. The auxiliary battery and generator system carried by the aircraft is to provide enough energy to reach the nearest electric charging station for the stranded vehicles. In cases such as disasters, the rapid delivery of health supplies can also be provided by this method. The aircraft designed for this purpose has a rotary wing and a feature that can change its body structure according to different load and weather conditions. The shape change improves its performance compared to conventional aircraft and increases its ability to fulfil its mission. For this purpose, the design of a shape-changing aircraft was realized.

Keywords: Octorotor UAV, Portable Battery, Cargo

Article History: Received:25.04.2024; Accepted:21.05.2024; Available online: 31.05.2024
How to Cite This Article: Özen, E., Oktay, T. (2024). Effect of Shape Change on Flight Performance of Eight Rotor Rotary Wing UAV .Volume 4, Issue 2, Energy, Environment and Storage, (2024), page 21-26.
Doi: https://doi.org/10.52924/ZQJP9091

1. INTRODUCTION

Unmanned aerial vehicles (UAVs), commonly known as drones, offer customers the advantage of speed, flexibility and convenience in delivering goods. They are particularly useful for tedious, dangerous or dirty tasks [1]. Delivery drones are unmanned aerial vehicles used to transport parcels, food, medicine or other goods. Due to the high demand for fast and efficient delivery, drone delivery system can be an effective solution for on-time deliveries and especially for emergency management [2]. "In recent years, significant progress has been made in various technologies designed for drone delivery of cargo. This progress has been primarily driven by industrial efforts. These deliveries can be by air, sea or land [3]. Shape-shifting drones can offer various advantages over conventional fixed structure drones and can become more effective for certain tasks [4]. The primary purpose of shape-shifting cargo drones is to increase the payload capacity. The drone's ability to change its shape enables it to carry loads of different sizes and weights more efficiently due to its changing geometry. This is especially important when large and heavy loads need to be transported. The drone's ability to change its shape increases its capacity to adapt to different missions. For example, it can be faster and more manoeuvrable for search and rescue operations, or more stable and safer for transporting medical supplies. Variable geometry can increase the drone's stability and adapt to different flight conditions. It can also increase the drone's maneuverability, improving its ability to fly in tight spaces. Shape-shifting cargo drones can be used for long-distance deliveries or urban deliveries. In these cases, it is important to transport large quantities of materials or packages quickly and efficiently. Such drones can contribute to advancing aviation technology. By developing innovative design and control systems, they can help shape the future of drone technology. Shape-shifting drones can consume less energy for certain missions, potentially leading to more environmentally friendly flights. This is an important advantage, especially in long-term or intensive use. Depending on the type of payload, multirotors can be effectively applied in a variety of missions, such as transportation, research, reconnaissance and life-saving. However, due to the nature of multirotor, the payload loaded on the multirotor is limited in terms of its location and weight. This limitation is a major disadvantage if the multirotor is used in various fields [15].

Electric vehicles continue to be an environmentally friendly and economical alternative. However, when vehicles need

*Corresponding author: enes.ozen@hku.edu.tr

to be charged during long journeys, a problem arises due to the lack of charging stations. To solve this problem, mobile charging station systems have been developed to meet the energy needs in emergency situations [5]. Another problem of electric cars is that battery performance decreases significantly in cold weather conditions. These situations can lead to vehicles remaining on the road longer than planned, causing disruptions to travel. These systems allow vehicles to be charged in emergency situations and thus prevent vehicles from being stranded. Mobile charging station systems consist of portable chargers. These devices are used to charge the batteries of vehicles. Mobile charging stations are designed to quickly charge the batteries of vehicles. In this way, vehicles are prevented from staying on the road and the safety of drivers is ensured. Offering a fast and effective solution for emergency access, mobile charging stations play an important role in meeting energy consumption, especially in long journeys or off-grid areas. These systems can be integrated with portable chargers and aerial vehicles, enabling access to electric vehicles from anywhere [6].

This paper presents the design of a deformable rotary wing aircraft, illustrated in Figure 1. The overall objective of the study is to discuss the design and geometry of the shape-shifting cargo drone (octorotor) in detail. Important features such as the body structure of the drone, the angle between the arms and their lengths are analyzed. The design and tuning of PID (Proportional-Integral-Derivative) controllers for controlling the drone's shape change are discussed. Advanced control systems for flight stability and safety are emphasized. The study emphasizes the variable geometry features designed to adapt the drone to different missions. These features optimize the payload, maneuverability and flight performance of the drone.

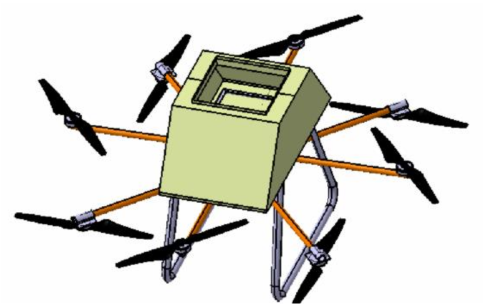

a)

b)

Fig. 1. a) Octorotor Unmanned Aerial Vehicle, **b)** Mobile Charging Station UAV

2. MATERIALS AND METHODS

2.1 General Structure and Components of Octorotor

The propulsion system of the rotary wing unmanned aerial vehicle consists of 8 rotors and propellers. The propellers rotate in opposite directions and the autopilot system on the aircraft controls the rotation speed of the propellers (Figure 2).

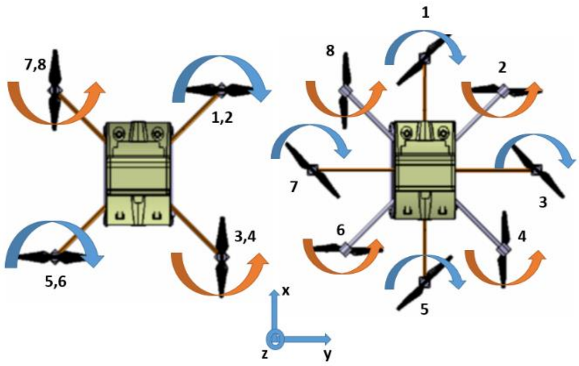

Fig. 2. Rotary Wing Aircraft Propeller Rotation Directions

Dynamic equations are obtained by using Newton Euler equations for modeling the aircraft system. Equation 1 is used to describe linear movements and equation 2 is used to describe angular movements. The octorotor has eight rotors and it is preferred that each rotor is equivalent. Rotors rotating at the same speeds create an upward force along the z-axis. The aircraft is stationary along the x and y axes and is considered to be in equilibrium. Rotation of the rotors at different speeds disrupts the equilibrium state in the x and y axes and the aircraft performs linear motion along the x, y and z axes and angular motion around these axes. These situations are expressed mathematically in equations 1 and 2.

$$F = ma \tag{1}$$

$$M = I\alpha \tag{2}$$

$$F_i = b\omega^2 ; i = 1,2,3,4,5,6,7,8 \tag{3}$$

Blade element theory is expressed in Equation 3. The rotation speed of the propellers is obtained by assuming that the air density, angle of attack and wing surface area are constants in the aerodynamic lift force equation. F_i is the equation that gives the aerodynamic force generated in each propeller. The U1 command is obtained by multiplying the square of the velocities of the rotors of the co-rotor by the coefficient b. When all the rotors of the aircraft with co-rotors rotate at the same speed, the ascent motion command input is obtained without any orientation as given in Equation 4. The b coefficient is calculated as a constant with the assumption that the aircraft is rotary winged, flies up to a certain altitude and the angles of attack of the propellers do not change, and is obtained from the engine-propeller manufacturer [7].

$$U_1 = b\left(\omega_1^2 + \omega_2^2 + \omega_3^2 + \omega_4^2 + \omega_5^2 + \omega_6^2 + \omega_7^2 + \omega_8^2\right) \quad (4)$$

The other command inputs to the octorotor are for pitch and roll motions and are given in equations 5 and 6. The input U2 required for pitching motion allows to realise angular motion around the x-axis. The speeds of the rotors on the right side of the x-axis are increased and the balance is disturbed. As a result, rolling moment is produced [8]. The speeds of the rotors in front with respect to the y-axis are increased and the balance is disturbed. A pitching moment is produced [9]. Generation of pitching and rolling moments and realisation of these movements are provided by U2 and U3 command inputs.

$$U_2 = bl\begin{pmatrix} \omega_5^2 \dfrac{\sqrt{2}}{2}\cos\alpha + \omega_6^2 \dfrac{\sqrt{2}}{2} + \omega_7^2 \dfrac{\sqrt{2}}{2}\cos\alpha + \omega_8^2 \dfrac{\sqrt{2}}{2} \\ -\omega_1^2 \dfrac{\sqrt{2}}{2}\cos\alpha - \omega_2^2 \dfrac{\sqrt{2}}{2} - \omega_3^2 \dfrac{\sqrt{2}}{2}\cos\alpha - \omega_4^2 \dfrac{\sqrt{2}}{2} \end{pmatrix} \quad (5)$$

$$U_3 = bl\begin{pmatrix} \omega_1^2 \dfrac{\sqrt{2}}{2}\sin\alpha + \omega_2^2 \dfrac{\sqrt{2}}{2} + \omega_7^2 \dfrac{\sqrt{2}}{2}\sin\alpha + \omega_8^2 \dfrac{\sqrt{2}}{2} \\ -\omega_5^2 \dfrac{\sqrt{2}}{2}\sin\alpha - \omega_6^2 \dfrac{\sqrt{2}}{2} - \omega_3^2 \dfrac{\sqrt{2}}{2}\sin\alpha - \omega_4^2 \dfrac{\sqrt{2}}{2} \end{pmatrix} \quad (6)$$

$$Q_i = d\omega_i^2; i = 1,2,3,4,5,6,7,8 \quad (7)$$

As the propellers rotate, they sweep the air and drag is created. This creates a moment opposite the direction of rotation. This value was expressed in equation 7. The parameters in the aerodynamic drag force equation are considered constant and are expressed with the coefficient d, considering that the aircraft can rise to a certain altitude and its speed has limits. The orientation movement of the quadrotor is provided by the U4 command input. Rotation of the propellers around the rotor axis creates torque due to drag. Since the rotors rotate at the same speed during ascent, 4 rotors rotate clockwise and 4 rotors rotate anti-clockwise, the total torque is zero. In helicopters, a tail rotor is also used to reset the torque produced by the propellers [10].

In Equation 8, the command input is given to generate the deflection moment [11]. In the equation given in Equation 7, the coefficient d is considered constant.

$$U_4 = d\left(\omega_1^2 - \omega_2^2 + \omega_3^2 - \omega_4^2 + \omega_5^2 - \omega_6^2 + \omega_7^2 - \omega_8^2\right) \quad (8)$$

2.2 Multi-rotor Aircraft Design with Variable Geometry

X8-Octo narrows laterally and longitudinally (in y and x directions) by changing the angle between its arms in the longitudinal axis direction [12]. The shape change is named as two different configurations; configuration 1L (octo), configuration 2L (X8).

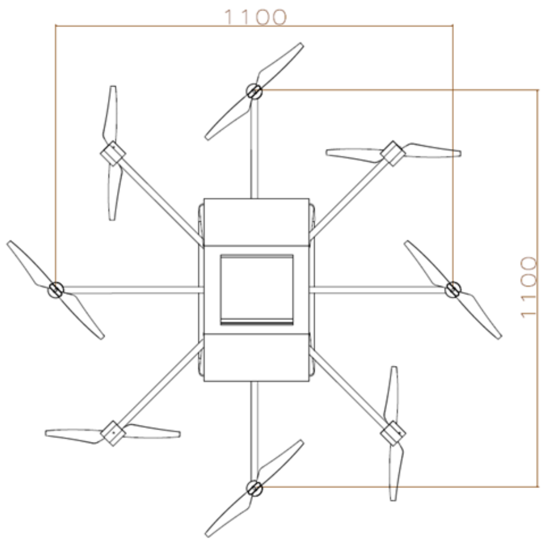

a)

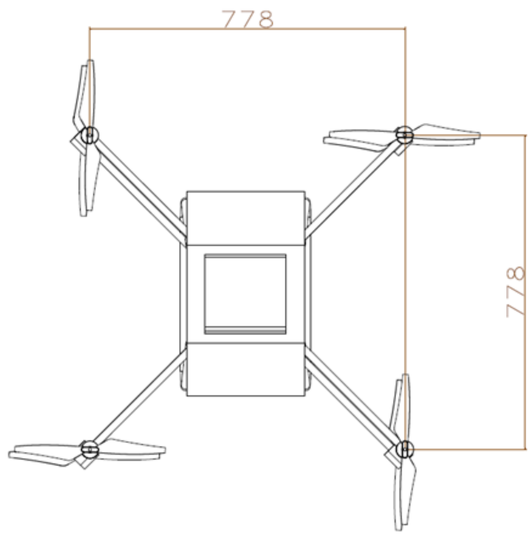

b)

Fig.3. Shape Changing Unmanned Aerial Vehicle **a)** Configuration 1L **b)** Configuration 2L

Changes in the geometry of the structure after the resulting shape change are given in Table 1.

Table 1. Dimensions of the Eight Rotor Aircraft

Aircraft Configuration	Width (mm)	Length (mm)
Configuration 1L	1100	1100
Configuration 2L	778	778

As seen in Eq.5 and 6, the distance of the rotor centre from the centre of gravity is effective in forward and lateral movements. These values will be taken into account when designing the controller in the next section.

The arms of the vehicle are lengthened and shortened and thus different configurations are created in different weather conditions. The shortening and lengthening of the arms also affect the flight performance values in previous studies [13]. The top view geometric dimensions of the aircraft in different configurations are shown in Figure 4.

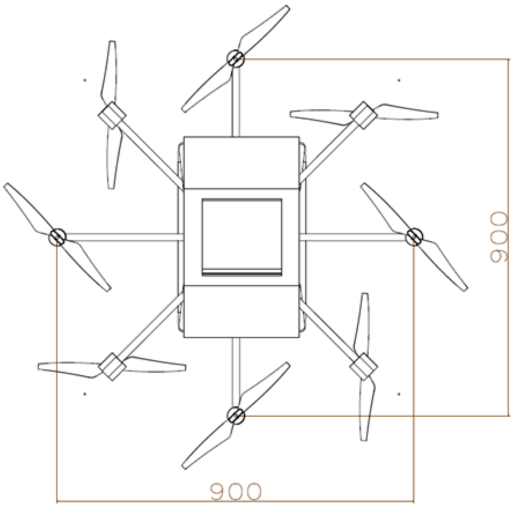

a)

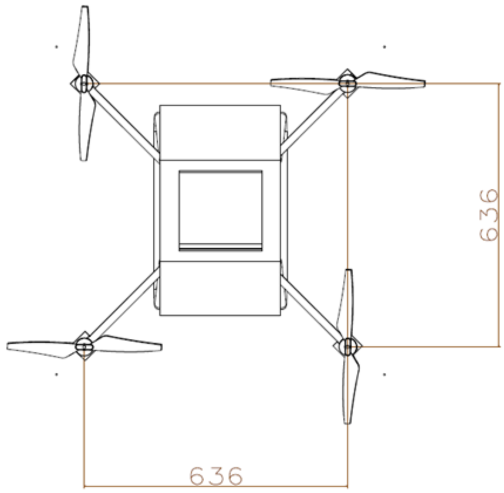

b)

Fig. 4. Shape Changing Unmanned Aerial **Vehicle a)** Configuration 3S **b)** Configuration 4S

The general characteristics of the 8-rotor aircraft before and after the shape change are given in Table 2.

Table 2. Octocopter Air Vehicle General Specifications

Aircraft Configuration	Width (mm)	Length (mm)
Configuration 3S	900	900
Configuration 4S	636	636

The stability and control behaviour of the aircraft differs in different configurations. In configuration 2, the vehicle has a narrow structure and is easier to control, while it is vulnerable to atmospheric disturbances. For this reason, when the wind speed is high, it turns into a more stable structure by extending its arms to increase wind resistance. In this case, manoeuvrability will decrease [13].

The change is realized by means of mechanisms in flight and on the ground. The signals received from the control system are transmitted to the relevant actuator and the angle between the arms is narrowed and widened and the arms are lengthened and shortened thanks to the screw-gear mechanism. The designed mechanism is given in Figure 5.

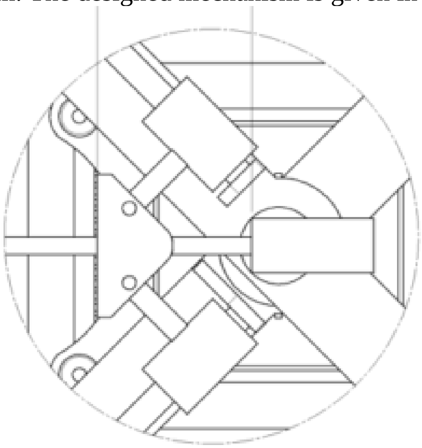

Fig.5. Mechanism enabling shape change

3. CONTROL SYSTEMS

3.1. Methods to Ensure Drone Stability during Shape Change

Aircraft perform 3 linear and 3 angular movements. It has 6 degrees of freedom mobility. According to this situation, the total forces and moments must be zero for the aircraft to remain in balance in the air. The commands that will ensure balance are control inputs. The rotary wing aircraft is controlled by both linear and angular accelerations. The aircraft uses the $U1$ command to ascend. It uses U2 command for roll motion (ϕ). It uses the U3 command for pitching motion (θ). Uses $U4$ command for yaw motion (ψ). 6 DOF says that there are 6 states for control but there are four control signals. The rotary wing aircraft is an incomplete actuator [16]. The aircraft performs the motion using elevation (z), roll (ϕ), pitch (θ) and yaw (ψ) commands. The control of the motion in the x and y direction is realized by the commands derived by the flight computer. When designing the aircraft controller, it can be divided into two subsystems. It controls the translational and angular motions of the aircraft. These are linear position, velocity and acceleration and angles, angular velocities and accelerations.

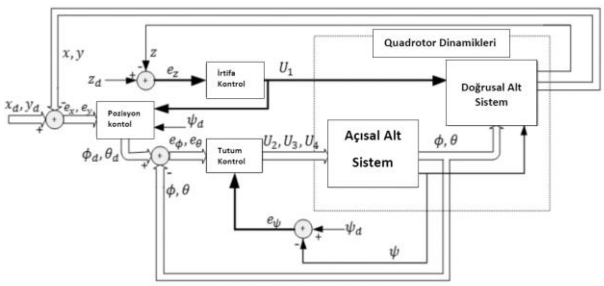

Fig. 5. Hierarchical Autopilot System Structure

As can be seen in the block diagram of the autopilot system, the differences between the desired data and the measured data are sent to the autopilot system via feedback. The PID controller processes this difference signal and adjusts the rotation speed of the engines to support stable flight.

4. RESULTS AND EVALUATION

In this study, a rotary wing aircraft was designed to deliver small cargo (10 desi / 2 kg) much faster in urban areas. The cargo may change the center of gravity of the aircraft, and in order to ensure control and stability of the aircraft in this case, a design is presented in which the arms can be extended and shortened and the belly angle can be changed. The fact that rotary wing aircraft are easy to use and require little maintenance, and that they do not need a runway for take-off and landing is an indication that they will be used more intensively in the future, and it is foreseen that the study can be used in systems that carry first aid supplies needed in emergency situations in larger capacities and can provide energy to electric vehicles in emergencies.

In this study, a design is presented to quickly meet the need for electrical energy in emergency situations. While DC-AC electric charging options of electric cars affect the time, DC electric energy method was preferred in this study. The biggest reason for this is the lightest solution for the electrical energy needed. With DC, cars will be able to gain 10 minutes of driving distance with 24 volt 7 kVA energy and 50Ah capacity battery and reach the nearest charging station [17].

Table 3. Charging Units and Features [17]

Charging Unit	Voltage	Current	Power Rating
House type	Single Phase	13-16-32 A	3-3,7—7,4 KVA
Normal	Single Phase	16 A	3,7 KVA
Fast	DC	up to 125 A	50 KW
	AC	up to 63 A	43 KVA

Higher capacity solutions can be offered with different portable energy sources. In future studies, larger aircraft with higher energy capacity will be designed by using the APU, which is also used in airplanes. Thanks to this system, the range of the aircraft will also increase significantly [18]. The design was prepared by examining similar aircraft that increase stability and controllability against different loads and variable weather conditions [19]. At this stage, it was concluded that the payload values presented could be transported safely.

5. CONCLUSION

In this study, improvements are presented by considering the disadvantages of cargo drones. These disadvantages include capacity limitations, range limitations, weather sensitivity, infrastructure requirements and legal barriers. The solutions to these problems; Compared to traditional cargo transportation, the carrying capacity of cargo drones is generally more limited, which can be improved by changing the shape. The flight range of cargo drones is directly related to battery life and payload capacity. Increased capacity provided a significant improvement to this problem. While bad weather conditions, especially strong winds and storms, can prevent cargo drones from operating safely and effectively, the advanced shape-shifting capability of the aircraft brings an important innovation. Cargo drones require appropriate infrastructure to operate. Infrastructure elements such as suitable landing and take-off areas, charging stations and logistics centers are important for cargo deliveries. Increased range and the ability to be used in emergencies, and the ability to take off and land vertically, are also important [20].

Disadvantages may hinder the widespread adoption of cargo drones or limit their use in certain application areas. However, with advances in technology and regulatory developments, these disadvantages may be overcome.

It is predicted that urban transportation will abandon traditional methods in favor of new approaches [21]. The aircraft structure designed and presented in this study appears to be well-suited for this anticipated shift.

REFERENCES

[1] Chiang, W. C., Li, Y., Shang, J., & Urban, T. L. (2019). Impact of drone delivery on sustainability and cost: Realizing the UAV potential through vehicle routing optimization. Applied energy, 242, 1164-1175.

[2] Seung-Hyun Seo, Jongho Won, Elisa Bertino, Yousung Kang, and Dooho Choi. 2016. A Security Framework for a Drone Delivery Service. In Proceedings of the 2nd Workshop on Micro Aerial Vehicle Networks, Systems, and Applications for Civilian Use (DroNet '16). Association for Computing Machinery, New York, NY, USA, 29–34. https://doi.org/10.1145/2935620.2935629

[3] Frachtenberg, E. (2019). Practical drone delivery. Computer, 52(12), 53-57.

[4] Özen, E. And Oktay, T. (2023). "Optimizing the Performance of an Unmanned Aerial Vehicle that can Detect and Avoid Obstacles." 9th International Zeugma Conference on Scientific Research, Gaziantep, Turkey, pp.1-5.

[5] Kerem, A. ve Gürbak, H. (2020). Elektrikli Araçlar İçin Hizli Şarj İstasyonu Teknolojileri. Gazi Üniversitesi Fen Bilimleri Dergisi Bölüm C: Tasarım ve Teknoloji, 8(3), 644-661. https://doi.org/10.29109/gujsc.713085

[6] Gönül, Ö., Duman, A. C., and Güler, Ö. (2021). Electric vehicles and charging infrastructure in Turkey: An overview. Renewable and Sustainable Energy Reviews, 143, 110913.

[7] Köse, O., Oktay, T. "Non Simultaneous Morphing System Design for Yaw Motion in Quadrotors," Journal of Aviation, vol. 3, no. 2, pp. 81-88, 2019.

[8] Bai, Y., Gururajan, S. Evaluation of a Baseline Controller for Autonomous “Figure-8” Flights of a Morphing Geometry Quadrotor: Flight Performance. MPDI/Drones 2019, 3, 70.

[9] Song, Q., Spall, J.C., Soh, Y.C. and Ni, J. “Robust neural network tracking controller using simultaneous perturbation stochastic approximation”, 2008, IEEE Transactions on NeuralNetworks, Vol. 19No. 5, pp. 817-835.
[10] Wallace, D. Dynamics and Control of a Quadrotor with Active Geometric Morphing. Master of Science in Aeronautics & Astronautics University of Washington, 2016.
[11] Oktay, T., Sal, F. Combined passive and active helicopter main rotor morphing for helicopter energy save. Journal of the Brazilian Society of Mechanical Sciences and Engineering, 2016, 38(6), 1511-1525.
[12] Uzun, M., Oktay, T. "Simultaneous UAV Having Actively Sweep Angle Morphing Wing and Flight Control System Design,” AIRCRAFT ENGINEERING AND AEROSPACE TECHNOLOGY, vol.95, no.1, pp.21-30, 2023.
[13] OKTAY, Tugrul, et al. Stochastic longitudinal autopilot tuning for best autonomous flight performance of a morphing decacopter. The Eurasia Proceedings of Science Technology Engineering and Mathematics, 2023, 23: 50-58.
[14] KÖSE, O., (2023). Yapay Sinir Ağları, PID ve Başkalaşım ile Octorotor Yanal Uçuş Kontrolü 4th International Black Sea Modern Scientific Research Congress (pp.79-90). Rize, Turkey
[15] Kim, C., Lee, H., Jeong, M., & Myung, H. (2021, September). A morphing quadrotor that can optimize morphology for transportation. In 2021 IEEE/RSJ International Conference on Intelligent Robots and Systems (IROS) (pp. 9683-9689). IEEE.
[16] Sariff, N. Ismail, Z.H., 2021. Broadcast event-triggered control scheme for multi-agent rendezvous problem in a mixed communication environment. Appl. Sci. 2021, 11, 3785.
[17] Karapinar, F., & Daldaban, F. (2022). Elektrikli Araçların Şarj Yöntemleri ve Şarj İstasyon Tipleri. Erciyes Üniversitesi Fen Bilimleri Enstitüsü Fen Bilimleri Dergisi, 38(3), 549-556.
[18] Özen, E., & Oktay, T., (2024). Elektrikli Araçların Acil Durumlarda Enerji İhtiyaçlari İçin Mobil Şarj İstasyonu Sistemi . Anadolu 14th International Conference on Applied Sciences (pp.1-10). Gaziantep, Turkey
[19]KÖSE, O., (2023). Başkalaşımın Octorotor Boylamasına Uçuşuna Etkisi. Black Sea Journal of Engineering and Science, vol.6, no.3, 185-192.
[20] Özen, E., & Oktay, T., (2024). Review of Cargo Drone Design and Capabilities. MAS 19 th International European Conference On Mathematics, Engineering, Natural & Medical Sciences (pp.1-10).
[21] Aydın, A.,Özen, E.,Öztürk, E. OtonomSistemlerin Şehir İçi Dağıtımiçin Uygulanabilirliği ve Ekonomide Yaratacağı Değerlerin İncelenmesi. 4. INTERNATIONAL 19MAYINNOVATIVESCIENTIFICAPPROACHESCONGRESS, Samsun, Türkiye, 20 -22Aralık 2020, ss.257-266

Energy, Environment and Storage

Journal Homepage: www.enenstrg.com

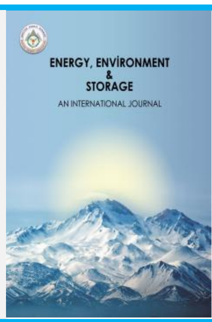

Experimental Investigation of the Effects of Biodiesel/Methanol Mixtures on Diesel Fuel on Engine Performance and Emission Values in a Diesel Engine

Alparslan Bozkurt[1*], Gürsel Çinar[2]

[1]*Department of Energy Systems Engineering, Erciyes University, Kayseri, Turkey. https://orcid.org/0000-0002-1532-0491*

[2]*Department of Mechanical Engineering, Erciyes University, Kayseri, Turkey.*

ABSTRACT. In internal combustion engines, operating conditions, engine design and fuel properties are closely related to efficiency. The alternative fuel used in diesel engines is expected to improve performance and emission values. Biodiesel is widely used to improve the fuel properties of alcohol and diesel. In this study, the effects of diesel, diesel-methanol, diesel-biodiesel, diesel-biodiesel-methanol mixtures are examined. Engine performance and exhaust emission tests were carried out on a three-cylinder, four-stroke diesel engine at a constant speed of 1500 rpm and five different loads: no load, 25%, 50%, 75% and 90%. Since constant speed and torque values could not be obtained in the no-load condition (T0) in the studies, the values at T0 were not used in the comparisons. As experimental data, thermal efficiency, CO, HC, CO2, NO emission values, in-cylinder pressure values and heat release rate values were examined. In experimental studies, the effects of adding different amounts of biodiesel and methanol on engine performance and emission values were compared with diesel. As a result of the comparison, positive results were obtained in the performance and gas emission values of alternative fuels compared to 100% diesel. In addition, fuel mixtures with biodiesel addition have better performance results than fuel mixtures with methanol addition.

Keywords: Energy, exergy, internal combustion engine, methanol fuel

Article History: Received:29.04.2024; Accepted:27.05.2024; Available online: 31.05.2024

Doi: https://doi.org/10.52924/KXEK8088

Nomenclature

100D	%100 Diesel
10B90D	%10 Biodiesel %90 Diesel
20B90D	%20 Biodiesel %80 Diesel
10M10B80D	%10 Methanol %10 Biodiesel %80 Diesel
10M10B80D	%10 Methanol %90 Diesel
CA	Crank Angle

1. INTRODUCTION

Today, constantly developing and growing main sectors such as industrialization, production and transportation mostly use fossil fuels as energy sources. Fossil fuels used as energy sources cause environmental and air pollution. In addition to its negative features such as environmental and air pollution, fossil fuel resources are also decreasing. Alternative fuel studies have gained importance due to the decrease in fossil fuels and the damage caused by exhaust gases to the environment [1-2]. While the studies reduce the harmful effects of exhaust gases, efficiency and performance are required to be acceptable. Many studies have been carried out to increase efficiency and reduce gas emissions in diesel engines. Some of these studies include the method of adding different additives to diesel used as fuel in diesel engines. [3-4]. The common goal of

*Corresponding author: alp52520@gmail.com

experiments using alternative fuels is to reduce the use of fossil fuels and to develop environmentally friendly alternative fuel types that can operate at equivalent or higher performance and efficiency than fossil fuels. There are studies in the literature in which biodiesel [5-7] and alcohol [8-10] are mixed as additives to diesel fuel in diesel engines, or biodiesel-alcohol [11-13] is mixed with diesel together. As a result, the fuel to be used as an alternative must be within acceptable limits in terms of both performance and environment. One of the most important factors affecting combustion in diesel engines is the properties of the fuel to be used [14-16]. In this study, 10% biodiesel, 20% biodiesel, 10% methanol and 10% biodiesel-10% methanol mixtures were added to diesel fuel. Properties of the fuel to be used in a diesel engine; It depends on properties such as cetane number, volatility, latent evaporation temperature, viscosity, surface tension of the fuel, and specific temperature of the fuel [17]. It has basic advantages such as being able to be used in diesel engines without the need for modification and having physicochemical properties like diesel [18-19]. In addition, it is frequently used in alternative fuel research due to its important features such as easy accessibility and producibility from many sources. There are studies using biodiesels obtained from different sources such as soybean [20], frying oil [21], waste oil [22], cottonseed [23], palm oil [24], animal [25] and vegetable [26] oils.

Another additive used in the study is methanol. The simplest component of the alcohol group is methanol. While methanol can be obtained from fossil-based fuels, it can also be obtained from sources such as biomass, wood and solid waste [27]. Therefore, methanol is an economical fuel. The fuel mixture obtained by adding methanol to diesel fuel can improve engine performance and emissions. For this reason, many researchers have carried out studies on the use of methanol as an alternative fuel in internal combustion engines. While methanol ($CH3OH$) is a pure substance, diesel fuel has a hydrocarbon structure. Fuel properties vary depending on the proportion of this hydrocarbon. The specific energy of methanol is lower than diesel. For this reason, methanol fuel mixtures have higher fuel consumption than diesel to reach the same power and torque values. Methanol is easy to produce and can be widely used as an alternative fuel because it is natural and less harmful to the environment. There is no need for any changes in the engine structure to use methanol as fuel in internal combustion engines [28]. Too much oxygen content. The lower combustion temperature causes the heat loss in the cylinder to decrease and therefore the thermal efficiency to increase. A lower flame temperature improves combustion and reduces NOx and CO [27-28].

Roy et al. [29] in the study, engine performance and emission values at high idle in a diesel engine with a biodiesel-diesel blend and a canola oil-diesel blend were compared. The fuels are mixed with diesel between 2-20%. As a result of the study, a decrease was observed in CO and HC emissions compared to pure diesel. Biodiesel-diesel and canola oil-diesel blends have higher fuel conversion efficiency than diesel. Cheung et al. [30] in their article, the engine performance and emission values of a low sulfur diesel-biodiesel mixture in a 4-cylinder engine at 1800 rpm were investigated experimentally. In the study, brake-specific fuel consumption and brake thermal efficiency increased. While HC and CO emissions decreased, NO emissions increased. Büyükkaya et al. [31] experimentally investigated the engine performance, emission and combustion of the mixture obtained by mixing the biodiesel obtained from pure rapeseed oil with diesel at 5%, 20% and 70% ratios. As a result of the experimental study, the use of biodiesel provided lower smoke opacity (60%) than diesel. He observed that the brake-specific fuel consumption (BSFC) increased by up to 11%. Utku et al. [32] in this study, the use of methyl ester obtained from waste frying oil as fuel was experimentally investigated. A turbocharged, four-cylinder, direct-injection diesel engine was used in the tests. Its results were compared with diesel fuel. As a result of the comparison, the specific fuel consumption is almost the same. In addition, emissions such as CO and CO have decreased. Asokan et al. [33] in this article, engine performance and emission parameters of linseed oil biodiesel were analyzed. Fuel mix compared to diesel. The resulting B20 has a BTE of 33.05%, which is higher at higher loads than diesel (33.43%). A significant reduction in emissions (CO, HC, NO, and smoke) was observed for linseed oil biodiesel blends compared to diesel fuel throughout the test. Yılmaz [28] in this study, biodiesel (45-40%), methanol (10-20%) and ethanol (10-20%) were added to diesel fuel at different rates and engine performance emission values were compared. Fuels created with biodiesel-alcohol-diesel additions have higher brake-specific fuel consumption compared to diesel. As the percentage of alcohol used in the mixtures increased, CO and HC emissions increased, while NO emission values decreased. Yasin et al. [34] in this study, engine performance and emission values of fuel mixtures obtained by adding 20% biodiesel 5%, and 10% methanol to diesel were compared with diesel. As a result of the tests, biodiesel-methanol-diesel mixtures increased brake-specific fuel consumption compared to diesel. As the amount of methanol in the mixture decreased, the NO emission value decreased and the CO emission value increased. Sayın et al. [35] in their experimental research, mixed methanol (5%, 10%, 15%) with diesel fuel in different proportions. The effect of the obtained fuel mixture on engine performance and emissions in a diesel engine was investigated. The experiments were carried out at 20 Nm engine load at 2200 rpm and three different injection pressures and timings. As a result of the experiments, it was observed that BSFC and BSEC increased in methanol-added fuels. He stated that this is due to the lower energy content of methanol. In addition, as the amount of methanol increased, BTE decreased. While fuels with methanol added decreased CO emission values, they increased NO emission values.

Qui et al. [41] in the study titled Performance and combustion characteristics of biodiesel–diesel–methanol blend fuelled engine. In his studies, he examined the effects of biodiesel and methanol-added diesel mixture on engine performance, gas emission data and combustion performance. 50% diesel and 50% biodiesel were used as base fuel. Experiments were carried out by adding 5% and 10% methanol to the resulting fuel. Experiments were carried out at different engine loads. As a result of the study, it was concluded that fuels with 1500 rpm methanol added at low engine power burned later than the base fuel. It has been stated that this delay time decreases as the engine load increases. When the cylinder pressure is compared, the cylinder pressure of methanol added fuels is higher than the base fuel. It was also stated that the fuel mixture using methanol contributes to the reduction of harmful gas emissions.

When the literature studies are examined, there are many articles using methanol and biodiesel mixtures as additives to diesel fuel. However, the number of studies comparing biodiesel and methanol mixtures together is less. This study, conducted at different torque values, will contribute to the literature in this context.

2. MATERIALS AND METHODS

2.1 The Experimental Setup

The experiments of the study were conducted at Erciyes University Engines Laboratory. The experiments are carried out three-cylinder, water-cooled, four-stroke diesel engine. The experimental setup also includes a hydraulic dynamometer, dynamometer load cell, encoder to measure engine speed, exhaust emission device for combustion gas emissions and smoke measurement, precision electronic scale to measure fuel consumption, piezoelectric pressure sensor, and temperature sensor measuring the temperature of the exhaust gases. Figure 1 and Table 1 show the experimental test system and the specifications of the diesel engine where the experiments are performed respectively.

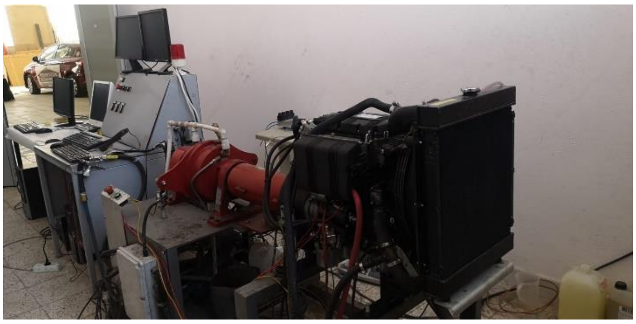

Fig. 1. Test Device

Table 1 Diesel Engine Specifications [36]

DİESEL ENGİNE	TECHNICAL SPECIFICATIONS
Cylinder number	3
Maximum speed (rpm)	3600
Maximum torque (Nm)	67
Compression ratio	22.8:1
Maximum power(kW)	19.5
Bore x Stroke (mm – mm)	75-77.6
Total cylinder volume (cm3)	1028

Table 2. Pressure Sensor Specifications [36]

Pressure Sensor	PCB113B22
Measurement Range	34475 KPa
Maximum Pressure	103425 KPa
Temperature Range	−73 to + 135 °C
Non-Linearity	≤1.0% FS
Sensitivity	0.145 mV/kPa
Low-Frequency Response	(−5%) 0.001 Hz
Resonant Frequency	>=500 kHz
Sensing Element	Quartz
Ranges	0–5000 psi
Accuracies	±1% of actual reading

The hydraulic dynamometer uses the NF150 model dynamometer, which can measure 0-6500 rpm engine speed and 0-450 Nm torque. As a hydraulic load cell, the CAS SBA 200L load cell is used and thus the effective engine torque is measured. Bosch BEA60 emission device has been used to measure the excess air ratio, hydrocarbon (HC), carbon monoxide (CO), carbon dioxide (CO2), nitrogen monoxide (NOx), and oxygen (O2) [37].

Table 3. Mixture of Fuels Used in Experiments

Alternative Fuels Used in Experiments	Diesel Mixing Ratio (%)	Biodiesel Mixing Ratio (%)
100D	100	-
10B90D	90	10
20B90D	80	20
10M90D	90	-
10M10B80D	80	10

2.2 Heat Release Rate Calculation

In internal combustion engine applications, heat release rate figures show where the heat appears, the duration of the heat, whether there is burning at different points, and how much heat must be given for pressure changes in the cylinder [36]. The heat release rate is calculated according to the first law of thermodynamics using the equation:

$$\frac{dQ_n}{d\theta} = \frac{\gamma}{\gamma-1} p \frac{dV}{d\theta} + \frac{1}{\gamma-1} V \frac{dp}{d\theta} \qquad (1)$$

In this formula, θ is the crank angle, γ (γ=Cp/Cv) is the specific heat ratio of the fuel/air mixture, and dQn/dθ is the net heat release [36].

3. Results and Discussion

3.1 Thermal Efficiency

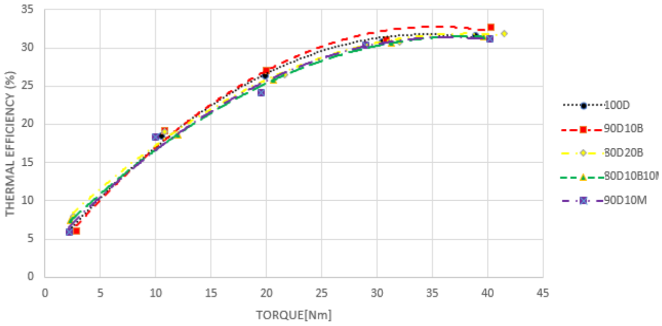

Fig.2. Thermal Efficiency Graph of Diesel, Biodiesel, Methanol Mixtures

The thermal efficiency graph of five different fuel mixtures is shown in Figure 2. According to the data obtained in the experiment, the highest thermal efficiency values were obtained with the use of 10% biodiesel in fuel mixtures. Biodiesel improves combustion in the cylinder due to its higher oxygen content and better C/O ratio compared to diesel [38]. Biodiesel Production and Engine]. The use of 20% biodiesel increased the thermal efficiency compared to diesel fuel, but it provided a lower increase than the use of 10% biodiesel. When the literature was searched, it was concluded that the use of 10% biodiesel has better results than the use of 20% biodiesel. As a result of the experiments we have done, the fact that 10% biodiesel gives better results than the use of 20% biodiesel overlaps with each other when compared with the literature. When the literature studies are examined, it is stated that better engine performance is obtained in the use of 10% biodiesel in some studies, while the use of 20%-50% in some studies gives better performance. The parameters that affect the performance most in the engine are compression ratio, injection advance, and air-fuel ratio. Air fuel ratio is the ratio of the amount of air to the amount of fuel. In order for combustion to occur, a certain amount of air and fuel must be present together in the combustion chamber. In order to obtain good performance data, all the fuel must be burned in the combustion chamber. The air-fuel ratio determines the quality of combustion and closely affects engine efficiency. In addition, the amount of oxygen in the biodiesel fuel improves combustion. There must be enough oxygen in the combustion chamber to burn all the fuel. Otherwise, unburned fuel will be expelled from the exhaust. This will both reduce engine performance and increase harmful emission gases released into the environment. Therefore, the amount of oxygen contained in additives such as biodiesel and methanol used in fuel mixtures will closely affect the efficiency. Each of these factors can be different in different engines, such as the injection advance, the shape of the combustion chamber, and the fuel-air mixture ratio. The viscosity value of the biodiesel fuel used in the study is higher than the diesel fuel. The higher the viscosity, the more energy the fuel needs to break down and evaporate. This is a factor limiting the increase in biodiesel rate. The high thermal efficiency of the %10 biodiesel mixture has a lower viscosity and increases the volatility compared to the %20 biodiesel mixture. This enhances the fuel atomization leading to improved air-fuel mixing [39]. At low compression ratios, a 10% biodiesel-added fuel mixture with lower viscosity yields better results than a 20% biodiesel fuel mixture with higher viscosity and a 10% biodiesel-added mixture. Therefore, the thermal efficiency for %20 biodiesel mixtures is lower than %10 biodiesel.[40] These results are consistent with the studies of ref 16 and 24. The use of 10% biodiesel increased the thermal efficiency by 2.6% in total at five different loads. The use of 20% biodiesel resulted in an improvement of 1.03%. The highest thermal efficiency in all fuel types was obtained at the maximum load of 40 Nm torque.

3.2 Gas Emission Values

In diesel engines, CO emission occurs due to an insufficient amount of oxygen in the combustion chamber and incomplete combustion. The increase in CO emissions is not a desirable situation for the emission parameters of diesel engines. The CO2 emission value is affected by the amount of oxygen contained in the fuel used in the engine, the air-fuel mixture ratio, the excess air factor and the turbulence in the combustion chamber. Increasing the CO2 emission value in engines is a desired result CO2 emission value increases as a result of good combustion in engines. NOX emission occurs due to the reaction of nitrogen in the air with oxygen at high temperatures resulting from combustion in engines. The higher the temperature in the cylinder, the higher the NOX emission. Different torque values have been obtained at 0% torque and a constant torque value could not be obtained. Therefore, test results at 0% load were not used when making comparisons.

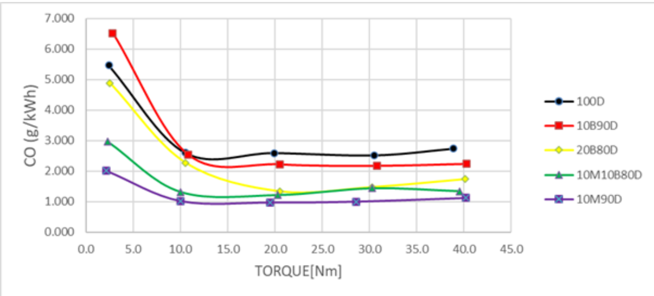

Fig. 3. CO Emission Graph of Diesel, Biodiesel, Methanol Mixtures

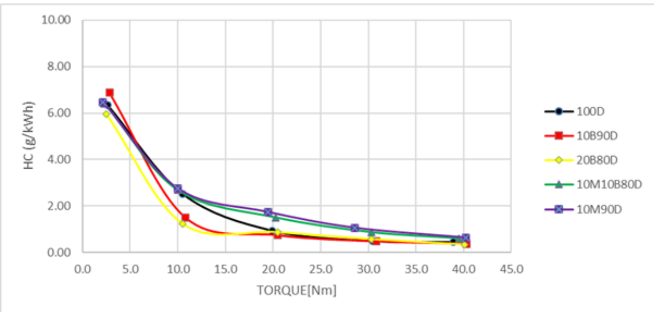

Fig. 4. HC Emission Graph of Diesel, Biodiesel, Methanol Mixtures

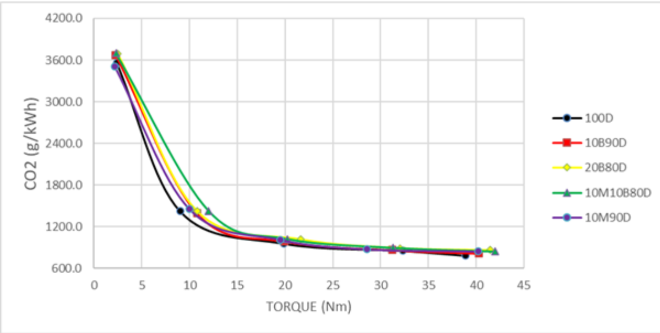

Fig. 5. CO_2 Emission Graph of Diesel, Biodiesel, Methanol Mixtures

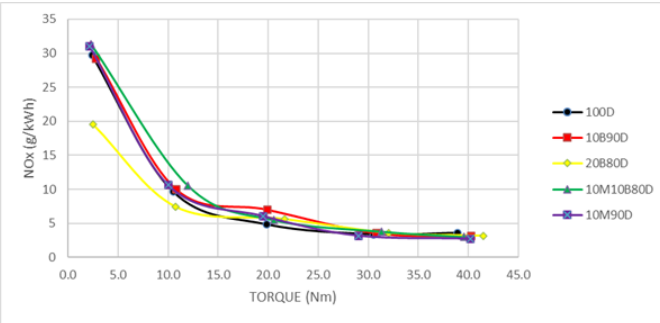

Fig. 6. NO_X Emission Graph of Diesel, Biodiesel, Methanol Mixtures

Figure 3 shows the CO emission graph of diesel biodiesel methanol blends. CO emission values vary between 6,525 g/kWh and 0,972 g/kWh. CO emission occurs due to incomplete combustion in the cylinder. Compared to 100D fuel, CO emission seems to decrease with the addition of biodiesel and methanol. In full load condition, 10B90D, 20B80D, 10M10B80D, and 10M90D fuels decreased their CO emission value by 17.92%, 36.60%, 50.92% and 59.00%, respectively, compared to 100D fuel. It has been observed that the high number of C atoms and oxygen density in the structure of biodiesel reduce the CO emission value. Methanol created a better air-fuel mixture during combustion due to the excess oxygen and low carbon in their structure compared with diesel and reduced the CO emission value.

Figure 4 shows the HC emission graph of diesel, biodiesel, and methanol blends. HC emission values decrease as the load value increases. Compared to pure diesel at full load, HC emission decreased respectively by 15.17% and 22.72% in 10B90D and 20B90D blends and increased respectively by 38.63% and 45.45% in 10M10B80D and 10M90D blends. Although HC emission decreases with the addition of biodiesel to diesel, HC emission increases when methanol is added. Since biodiesel makes the combustion more ideal, HC emission decreases, while HC emission increases due to the low cetane numbers of methanol. Adding 20% biodiesel resulted in a greater reduction in HC emissions than adding 10%. Figure 5 shows the CO2 emission graph of the mixtures obtained using diesel, biodiesel, and methanol. Effects such as the air excess coefficient, the turbulence occurring in the combustion chamber and the chemical properties of the fuel vary the amount of CO2. In general, higher CO2 emissions mean better combustion. When the figure is examined, CO2 emissions increase in all fuel mixtures compared to diesel fuel in full load conditions. This is because methanol and biodiesel contain more oxygen in their structures compared to diesel. A high CO2 emission value at full load has been obtained in the 90D10M mixture. The lowest CO2 emission value at full load was obtained in pure diesel fuel. CO2 and CO emissions are inversely proportional to each other. In a good combustion, CO2 emission increases while CO emission value decreases.

Figure 6 shows the NOx emission graph of the mixtures obtained using diesel, biodiesel, and methanol. NOx emission gas is formed by the reaction of nitrogen in the air with oxygen at high temperatures. NOx gas emission is affected by effects such as combustion reaction time, gas temperature in the cylinder and the amount of oxygen. In general, to reduce NOx emission, the temperature formed during combustion in the cylinder should be reduced. When the figure is examined, it has been observed that the methanol fuels reduce the NOx emission value compared to the normal diesel fuel. The reason for the lower NOx emission of methanol fuel blends: Methanol absorbs heat from the cylinder due to high evaporation heat and lowers the temperature in the cylinder. Thus, a lower in-cylinder temperature is achieved and less NOx emissions are produced.

3.3 In-Cylinder Pressure and Heat Release Rate

In-cylinder pressure and thermal release values help us to comment on the performance of a diesel engine. It gives information about how performance emerges, along with fuel consumption and engine efficiency. The position of the maximum pressure points and the in-cylinder pressure curve is important when interpreting engine performance. The size of the area under the in-cylinder pressure curve is related to the engine efficiency.

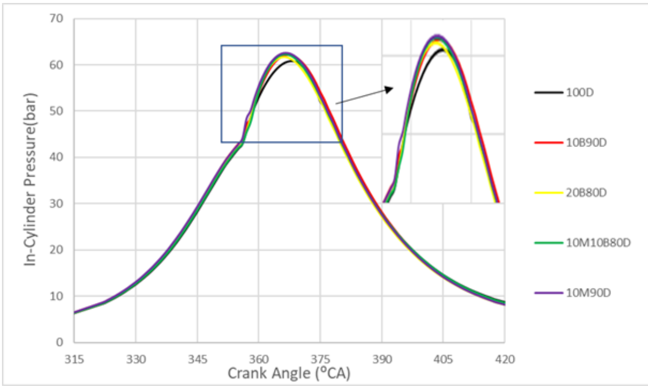

Fig. 7. In-cylinder pressure Graph of Diesel, Biodiesel, and Methanol Mixtures at T40 Load Value

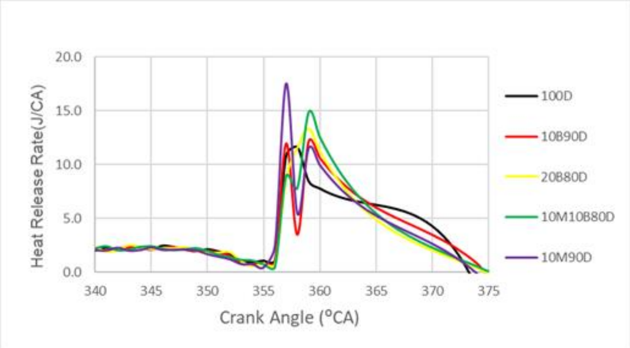

Fig. 8. Heat Release Rate Variation with Crankshaft Angle

In-cylinder pressure graph for diesel, biodiesel, and methanol blends at T40 (40 Nm torque) load value is shown in Figure 7. The change in heat release rate with the crankshaft angle is shown in Figure 8. The highest in-cylinder pressure values were obtained in the 10M90D mixture at 62.59 bar. Due to the rapid evaporation of methanol, the pressure in the methanol mixtures increased rapidly in the cylinder and then decreased. In-cylinder pressure values for 100D have 60.82 bar at 368 CA, for 10B90D 62.09 bar at 367 CA, for 20B80D 61.62 bar at 366 CA, for 10M10B80D 62.225 bar at 366 CA, and for 10M90D 62.59 bar at 367 CA. In the case of full load, the in-cylinder pressure values increased with the addition of biodiesel (10B90D, 20B80D) and methanol (10M10B80D, 10M90D) added to the diesel by volume. When the heat release rate is examined, it is seen that the heat release rate of methanol and biodiesel mixtures is larger than diesel fuel. It is thought that the heat release rate is higher than diesel because the mixtures burn faster than normal diesel fuel. When Figure 8 is examined, the heat release rate increased when biodiesel and methanol were added to pure diesel. The highest heat release rate was obtained with a mixture of 17.54 J/CA 10M90D at 357 CA. Due to the rapid evaporation of methanol, a sudden heat is generated in the cylinder when the spraying starts, but it has been observed that the temperature drops rapidly afterwards.

4. CONCLUSION

In this study, the effect of mixing biodiesel and methanol with diesel fuel on engine performance and emission values was investigated. The results of this study can be summarized as follows:

1-In the experiments where diesel methanol and biodiesel mixtures were used, the highest thermal efficiency values were obtained in the 10B90D mixture (10% biodiesel, 90% diesel) with a ratio of 32.75% at full load. When the 10B90D fuel mixture is compared to the 100D fuel mixture, the thermal efficiency increases by 3.61%. These results are consistent with references 39 and 40.

2-Since methanol has lower thermal energy than biodiesel and diesel, lower performance results were obtained compared to biodiesel and diesel.

3-The fuels obtained at the end of the mixture contributed to the improvement of harmful gas emissions compared to diesel.

4-Fuel mixtures were applied without making any changes to the engine and the results were obtained.

Acknowledgments

The authors would like to acknowledge Erciyes University, for the Scientific Research Projects Unit of Erciyes University, Turkey, for the financial support under the grant number FYL-2021-10787.

REFERENCES

[1] Akansu, S. O., Dulger, Z., Kahraman, N., & Veziroğlu, T. N. (2004). Internal combustion engines are fueled by natural gas—hydrogen mixtures. International journal of hydrogen energy, 29(14), 1527-1539.

[2] Wei, J., & Wang, Y. (2021). Effects of biodiesels on the physicochemical properties and oxidative reactivity of diesel particulates: A review. Science of The Total Environment, 788, 147753. https://doi.org/10.1016/j.scitotenv.2021.147753

[3] Bae, C., & Kim, J. (2017). Alternative fuels for internal combustion engines. Proceedings of the Combustion Institute, 36(3), 3389-3413. https://doi.org/10.1016/j.proci.2016.09.009

[4] Örs, I., Sarıkoç, S., Atabani, A. E., Ünalan, S. E. B. A. H. A. T. T. İ. N., & Akansu, S. O. (2018). The effects on performance, combustion and emission characteristics of DICI engine fuelled with TiO2 nanoparticles addition in diesel/biodiesel/n-butanol blends. Fuel, 234, 177-188. https://doi.org/10.1016/j.fuel.2018.07.024

[5] Nabi, M. N., Akhter, M. S., & Shahadat, M. M. Z. (2006). Improvement of engine emissions with conventional diesel fuel and diesel–biodiesel blends. Bioresource Technology, 97(3), 372-378.

[6] Mamedov, I., Musazade, M., Rustamova, H., (2023). Testing of Some Ionic Liquids at the Synthesis of Biodiesel, Environment and Storage, 3(1). https://doi.org/10.52924/PGZS3445

[7] Zhu, L., Cheung, C. S., Zhang, W. G., & Huang, Z. (2011). Combustion, performance and emission characteristics of a DI diesel engine fueled with ethanol–biodiesel blends. Fuel, 90(5), 1743-1750.

[8] Kumar, S., Cho, J. H., Park, J., & Moon, I. (2013). Advances in diesel–alcohol blends and their effects on the performance and emissions of diesel engines. Renewable and Sustainable Energy Reviews, 22, 46-72.

[9] Kul, V. S. (2023). Experimental Investigation of the Effect of Acetone Additive to Diesel Fuel on Engine Performance and Exhaust Emissions at Partial Loads. Energy, Environment and Storage, 3(1).

[10] Emiroğlu, A. O., & Şen, M. (2018). Combustion, performance and emission characteristics of various alcohol blends in a single cylinder diesel engine. Fuel, 212, 34-40.

[11] Tse, H., Leung, C. W., & Cheung, C. S. (2015). Investigation of the combustion characteristics and particulate emissions from a diesel engine fueled with diesel-biodiesel-ethanol blends. Energy, 83, 343-350.

[12] Ağbulut, Ü., Sarıdemir, S., & Albayrak, S. (2019). Experimental investigation of combustion, performance and emission characteristics of a diesel engine fuelled with diesel–biodiesel–alcohol blends. Journal of the Brazilian Society of Mechanical Sciences and Engineering, 41(9), 389.

[13] Ghadikolaei, M. A., Cheung, C. S., & Yung, K. F. (2018). Study of combustion, performance and emissions of diesel engine fueled with diesel/biodiesel/alcohol blends having the same oxygen concentration. Energy, 157, 258-269.

[14] Ra, Y., Reitz, R. D., Mcfarlane, J., & Daw, C. S. (2009). Effects of fuel physical properties on diesel engine combustion using diesel and bio-diesel fuels. SAE International Journal of Fuels and Lubricants, 1(1), 703-718.

[15] Geng, P., Cao, E., Tan, Q., & Wei, L. (2017). Effects of alternative fuels on the combustion characteristics and emission products from diesel engines: A review. Renewable and Sustainable Energy Reviews, 71, 523-534.

[16] Kidoguchi, Y., Yang, C., & Miwa, K. (2000). Effects of fuel properties on combustion and emission characteristics of a direct-injection diesel engine. SAE transactions, 1149-1157.

[17] Hills, F. J., & Schleyerbach, C. G. (1977). Diesel fuel properties and engine performance (No. 770316). SAE Technical Paper.

[18] Benjumea, P., Agudelo, J., & Agudelo, A. (2008). Basic properties of palm oil biodiesel–diesel blends. Fuel, 87(10-11), 2069-2075 https://doi.org/10.1016/j.fuel.2007.11.004

[19] Saxena, P., Jawale, S., & Joshipura, M. H. (2013). A review on prediction of properties of biodiesel and blends of biodiesel. Procedia Engineering, 51, 395-402. https://doi.org/10.1016/j.proeng.2013.01.055

[20] Alcantara, R., Amores, J., Canoira, L. T., Fidalgo, E., Franco, M. J., & Navarro, A. (2000). Catalytic production of biodiesel from soy-bean oil, used frying oil and tallow. Biomass and bioenergy, 18(6), 515-527. https://doi.org/10.1016/S0961-9534(00)00014-3

[21] Encinar, J. M., Gonzalez, J. F., & Rodríguez-Reinares, A. (2005). Biodiesel from used frying oil. Variables affecting the yields and characteristics of the biodiesel. Industrial & Engineering Chemistry Research, 44(15), 5491-5499. https://doi.org/10.1021/ie040214f

[22] Hajjari, M., Tabatabaei, M., Aghbashlo, M., & Ghanavati, H. (2017). A review on the prospects of sustainable biodiesel production: A global scenario with an emphasis on waste-oil biodiesel utilization. Renewable and Sustainable Energy Reviews, 72, 445-464. https://doi.org/10.1016/j.rser.2017.01.034

[23] Rashid, U., Anwar, F., & Knothe, G. (2009). Evaluation of biodiesel obtained from cottonseed oil. Fuel Processing Technology, 90(9), 1157-1163. https://doi.org/10.1016/j.fuproc.2009.05.016

[24] Mekhilef, S., Siga, S., & Saidur, R. (2011). A review on palm oil biodiesel as a source of renewable fuel. Renewable and Sustainable Energy Reviews, 15(4), 1937-1949. https://doi.org/10.1016/j.rser.2010.12.012

[25] Banković-Ilić, I. B., Stojković, I. J., Stamenković, O. S., Veljkovic, V. B., & Hung, Y. T. (2014). Waste animal fats as feedstocks for biodiesel production. Renewable and sustainable energy reviews, 32, 238-254.

[26] Mamedov, I., Mamedov, G., Azimova, N., (2022). Testing of Ethylene Glycol Ketal, Dioxane and Cyclopentanone as Components of B10, B20 Fuel Blends, Environment and Storage, 2(1). https://doi.org/10.52924/RBCY7188

[27] Yao, C., Cheung, C. S., Cheng, C., Wang, Y., Chan, T. L., & Lee, S. C. (2008). Effect of diesel/methanol compound combustion on diesel engine combustion and emissions. Energy conversion and management, 49(6), 1696-1704. https://doi.org/10.1016/j.enconman.2007.11.007

[28] Yilmaz, N. (2012). Comparative analysis of biodiesel–ethanol–diesel and biodiesel–methanol–diesel blends in a diesel engine. Energy, 40(1), 210-213. https://doi.org/10.1016/j.energy.2012.01.079

[29] Roy, M. M., Wang, W., & Bujold, J. (2013). Biodiesel production and comparison of emissions of a DI diesel engine fueled by biodiesel–diesel and canola oil–diesel blends at high idling operations. Applied Energy, 106, 198-208. https://doi.org/10.1016/j.apenergy.2013.01.057

[30] Di, Y., Cheung, C. S., & Huang, Z. (2009). Experimental investigation on regulated and unregulated emissions of a diesel engine fueled with ultra-low sulfur diesel fuel blended with biodiesel from waste cooking oil. Science of the total environment, 407(2), 835-846. https://doi.org/10.1016/j.scitotenv.2008.09.023

[31] Buyukkaya, E. (2010). Effects of biodiesel on a DI diesel engine performance, emission and combustion characteristics. Fuel, 89(10), 3099-3105 https://doi.org/10.1016/j.fuel.2010.5.034

[32] Utlu, Z., & Koçak, M. S. (2008). The effect of biodiesel fuel obtained from waste frying oil on direct injection diesel engine performance and exhaust emissions. Renewable energy, 33(8), 1936-1941. https://doi.org/10.1016/j.renene.2007.10.006

[33] Asokan, M. A., Prabu, S. S., Prathiba, S., Akhil, V. S., Abishai, L. D., & Surejlal, M. E. (2021). Emission and performance behaviour of flax seed oil biodiesel/diesel blends in DI diesel engine. Materials Today: Proceedings, 46, 8148-8152. https://doi.org/10.1016/j.matpr.2021.03.108

[34] Yasin, M. H. M., Mamat, R., Yusop, A. F., Aziz, A., & Najafi, G. (2015). Comparative study on biodiesel-methanol-diesel low proportion blends operating with a diesel engine. Energy Procedia, 75, 10-16. https://doi.org/10.1016/j.egypro.2015.07.128

[35] Sayin, C., Ozsezen, A. N., & Canakci, M. (2010). The influence of operating parameters on the performance and emissions of a DI diesel engine using methanol-blended-diesel fuel. Fuel, 89(7), 1407-1414.

[36] İlhak, M. İ., Doğan, R., Akansu, S. O., & Kahraman, N. (2020). Experimental study on an SI engine fueled by gasoline, ethanol, and acetylene at partial loads. Fuel, 261, 116148. https://doi.org/10.1016/j.fuel.2019.116148

[37] Fil, H. E., Akansu, S. O., & Ilhak, M. I. (2022). Experimental assessment on performance, emission and combustion characteristics of the use of diesel-acetylene mixtures at different loads in a ci engine. Fuel, 324, 124469. https://doi.org/10.1016/j.fuel.2022.124469

[38] Sarıkoc. S., 2019. "Investigation of Effects of Hydrogen and Titanium Dioxide Addition to Biodiesel-Butanol-Diesel Mixtures on Performance and Emission Parameters", Ph.D. Thesis, Erciyes University Institute of Science, Kayseri

[39] Ong, H.C., Masjuki, H.H., Mahlia, T.M.I., Silitonga, A.S., Chong, W.T., Leong, K.Y., Optimization of Biodiesel Production and Engine Performance from High Free Fatty Acid Calophyllum Inophyllum Oil in CI Diesel Engine, Energy Conversion and Management, 81

[40] Soysal C., 2008. "Experimental Investigation of the Effect of Using Biodiesel-Diesel Fuel Mixtures on Engine Performance in Diesel Engines", M.Sc., Karadeniz Technical University, Institute of Science and Technology, Trabzon.

Energy, Environment, and Storage

Journal Homepage: www.enenstrg.com

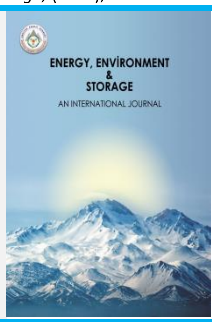

Gravity Energy Storage Technologies: A Review of the Solid Gravity Energy Storage Applications

Selda Aslan[1*], Sezai Alper Tekin [2], Recep Emir [3]

[*1,2]Department of Industrial Design Engineering, Erciyes University, Kayseri, Turkey, ORCID:* [1]0009-0009-8664-7780, [*2]0000-0001-5860-2758

[3]Department of Electrical and Electronics Engineering, Erciyes University, Kayseri, Turkey, ORCID: [3]0000-0001-5860-2758

ABSTRACT. The usage of renewable energy sources is increasing to reduce the carbon footprint. Renewable energy sources provide limited electricity generation and cannot meet the variable energy demand. Large-scale energy storage systems are needed for sustainability. The applicability of energy storage technology depends on many factors such as energy source, site availability, energy density, storage time, storage capacity, system cost, environmental impact, reliability, durability, and system integration capacity. Solid gravity storage technology is a promising new alternative in large-scale energy storage. There are various types of SGES systems classified according to the application method. In this paper, studies on various SGES methods are reviewed. Studies on the applicability factors of SGES systems and their integration into the electricity grid are evaluated. SGES technology has advantages in terms of geographical compatibility, storage volume, security, and energy conversion efficiency. It has been observed that successful results have been obtained in the theoretical studies. However, there is a need for the development of physical simulations and more comprehensive techno-economic analyses.

Keywords: Sustainability, Renewable Energy, Energy Storage Technologies, Solid Gravity Energy Storage

Article History: Received:30.04.2024; Accepted:30.05.2024; Available online: 31.05.2024
Doi: https://doi.org/10.52924/CKEX2410

1. INTRODUCTION

Meeting the energy demand is an important situation to solve in today's world. The depletion of fossil fuels and the harm they bring about the outdoors are facts that cannot be ignored. The usage of renewable energy resources is increasing in line with the goals of sustainability and carbon footprint reduction for the Green World [1]. The fact that renewable energy production methods cannot provide continuous production and the amount of energy demanded is unpredictable has made it necessary to develop energy storage systems to be used when required [2]. The difference between the amount of energy production and consumption is consistently changing. In this context, energy storage systems are of great importance as they can be used when needed and have critical importance in sustainability [3]. The applicability of energy storage systems depends on their certain characteristics. These characteristics are indicative of the overall quality, long-term sustainability, and successful applicability of the systems. Applicability of an energy storage system; It depends on many factors such as energy source, site availability, energy density, storage duration, storage capacity, system cost, environmental impact, reliability, durability, and system integration capacity [4]. Today, the biggest type of energy needed is electrical energy, and the focus of many studies is on the storage of electrical energy [5]. Wind and solar energy sources require an energy storage system due to intermittent energy production. These systems increase the power stability of the generated energy and ensure its integration into the grid and frequency and voltage management. These systems increase the power stability of the energy produced and provide network integration, frequency, and voltage management [6]. Various energy storage methods are utilized to store energy in different types and convert it into electricity when necessary. None of the developed energy storage technologies can fully meet the required characteristics [7]. For this reason, it is important to compare energy storage systems according to the purpose of the planned application of the system to be selected and analyze the applicability factors in detail [8]. A very important prerequisite for sustainable and clean energy solutions is the further development of large-scale energy storage technologies.

2. GRAVITY ENERGY STORAGE TECHNOLOGIES

Energy storage technologies; it is classified under 5 main headings according to the energy storage form: electrochemical, electrical, chemical, mechanical, and thermal. Among those forms, mechanical energy storage methods are classified under three subheadings: kinetic

*Corresponding author: slda.asln@gmail.com

energy storage, elastic potential energy storage, and gravitational potential energy storage technologies.

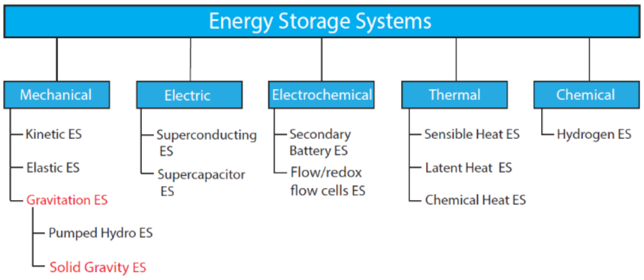

Fig. 1. Energy storage classification

Gravitational energy storage (GES) technology uses the power of gravity to store electrical energy. Although GES technology is considered a new method, it has been used in dams and hydroelectric power plants long since with the pumped hydro energy storage technology (PHES) method. It has been observed that in many of the studies examined, Solid gravity energy storage technology (SGES) is referred to as GES. But GES technology includes not only the use of solid weights but also PHES technology.[9] SGES technology is seen as an innovative and promising new solution method for storing large-scale renewable energies. PHES technology has difficulties arising from geographical limitations and the use of water as a heavy material. In contrast, a Solid Energy Storage System (SGES) is more advantageous compared to PHES in terms of geographical compatibility, energy density, and efficiency. SGES provides a more economical solution by using high-density solids as a heavy material. Compared to the commonly used Battery Energy Storage System (BES) and Hydroelectric Energy Storage (HES) technologies, SGES is safer and superior in terms of grid synchronization and inertia. This superiority helps the stable operation of power systems containing high amounts of renewable energy. Compared to Liquid Air Energy Storage (LAES), although SGES has less energy density, it has higher cycle efficiency. Thus, SGES has wide application potential in regions that are not suitable for PHES but have rich access to renewable energy sources and is considered an alternative solution to PHES. [10] In this article, studies on GES technology methods and the applicability factors of SGES technology, which is a new energy storage method, are evaluated.

3. TYPES OF SGES TECHNOLOGY

Unlike other systems that require a specific landform, SGES has various methods that can be adapted to geographical regions. SGES has emerged as an alternative and complementary method to overcome this problem. Different models of SGES are distinguished based on the solid energy storage media, transport methods, and platforms used.

3.1 Tower solid gravity energy storage (T-SGES)

The T-SGES method was developed by the Energy Vault Company. The system consists of a central tower with six lifting arms. The arms are capable of lifting concrete blocks 120 meters high and weighing 35 tonnes. These blocks, used for energy storage purposes, are stored as potential energy by stacking or dismantling regularly on the tower. The theoretical energy storage capacity of the system is 35 MWh and can quickly provide a maximum power of 4 MW to the electric grid; This can happen in as little as 2.9 seconds. Energy conversion efficiency can reach up to 96% and the concrete blocks used can be obtained from local sources and adapted to different geographies. The electricity production cost was determined as 44.58 dollars/MWh. In 2023, Energy Vault developed a project with 100 MWh storage capacity and 25 MW generation capacity in Zhejiang in cooperation with China Tianying Company [11].

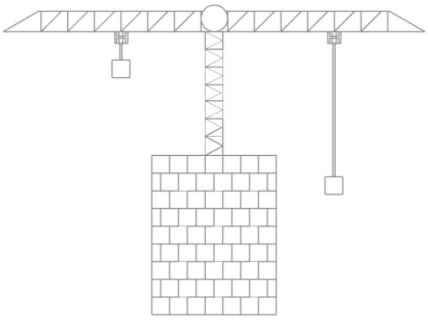

Fig. 2. Tower solid gravity energy storage

The capacity of the T-SGES system is directly proportional to brick mass and tower height. As height increases, storage capacity increases quadratically. However, an increase in height also increases system costs and technical requirements, so the tower height usually does not exceed 120 meters. Brick quality is related to the needs of the robot arm and system performance, and as quality increases, costs generally decrease while technical requirements increase. The output and discharge power of the system depends on the brick mass and the downstream speed; speed adjustments are a cost-effective way to increase the power capacity. The downstream velocity is proportional to the height, which sets the power limit, and meeting power requirements and height standards are essential for system effectiveness [12].

3.2 Shaft solid gravity energy storage (S-SGES)

Gravitricity, a company based in Scotland, has developed an innovative shaft model. This model can produce energy from 1 MW to 20 MW, using huge rocks weighing between 500 and 5000 tons, with a system with a total capacity of 12,000 tons [13]. This system can provide energy for periods ranging from 5 minutes to 8 hours and has an efficiency rate of 80% to 90%. The company has enabled the system to reach maximum power with a mechanism that can lift and lower a 50-ton load in 11 seconds. Gravitricity, which built a 0.25 MW capacity demonstration facility in Edinburgh in 2021, started a 2 MWh capacity energy storage project in Europe in 2022. SGES technology offers advantages such as long life, fast response time, and flexibility in operating modes. It also operates at a much lower cost than lithium batteries. However, the system faces several challenges. These include steel cable unraveling due to insufficient torque, shaking and turning of heavy loads, and insufficient crane capacity. [14] Gravity Power Company developed a solar energy method using abandoned mines in 2011. The main distinguishing point of this method is the usage of stone instead of water as the energy storage medium. [15] In 2020, the China University of Mining and Technology aimed to increase energy storage capacity by using two abandoned mines and building channels at different heights between these mines. This approach optimizes the release of potential energy during operation while facilitating the horizontal transport and storage of heavy objects. [16]

3.3 Piston solid gravity energy storage (P-SGES)

The P-SGES system consists of various components that play critical roles in energy storage and conversion processes. First of all, the gravity piston is positioned in a water-filled chamber, enabling the conversion of electrical energy into potential energy. This process is managed by the engine-generator and pump-turbine units, and in case of excess energy, it is carried out by pumping water and elevating the piston. Energy storage capacity is directly related to the dimensions, efficiency, and friction factors of the piston. The system has the potential to increase energy density and efficiency by using high-density materials. [17]

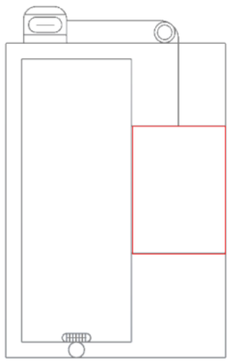

Fig. 3. Piston solid gravity energy storage

Research by Berrada and others. indicates that using steel or concrete to seal energy storage containers is more effective. American companies such as Gravity Power, which have adopted this technology, have shown the fact that the energy storage capacity of P-SGES systems can reach decades of megawatt hours, can be activated in milliseconds and react in seconds at full power, and can also provide uninterrupted energy for four hours and can reach 5 MW with an efficiency of 75-80%. It shows that it can produce nominal power. A project proposed by Heindl Energy aims to hydraulically lift a large rock mass and store potential energy. By discharging pressurized water through turbines, energy storage capacity is increased. The project states that energy storage capacity may vary between 1 MWh and 10 MWh and investment costs may range between \$120,000/MWh and \$380,000/MWh. The solar power system proposed by Zhang in 2018 increases efficiency by integrating shaft energy storage with pumped storage. [18]

3.4 Mountain Cable-Car solid gravity energy storage (MC-SGES)

In the MC-SPP system, the height of the mountain is used for the conversion and storage of gravitational potential energy and electrical energy, which enables more efficient use of mountain resources. To store energy, heavy objects are transported from the foot of the mountain to its summit with the help of a cable car; there is an electric motor and generator here. The descent of heavy objects with the help of gravity makes it possible to produce electricity through a generator. MC-SGES offers a safer alternative with more regular charging and discharging processes compared to tower-type energy storage systems. [19]

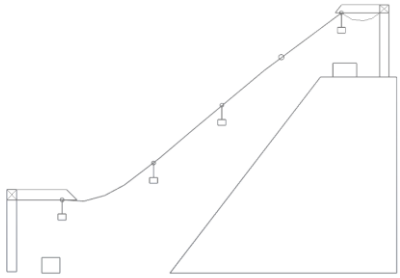

Fig. 4. Mountain Cable-Car solid gravity energy storage

Energy storage capacity and efficiency vary depending on factors such as altitude difference and engine efficiency. The height difference in projects is generally between 200 and 2000 meters, which affects load losses between 90% and 97%. While engine efficiency varies between 75% and 95%, storage efficiency has a value between 68% and 92%. Round-trip efficiency varies between 46% and 85%, and an efficiency above 75% is essential to achieve economic advantage. The output power for MGES is directly related to the time spent. Considering the relationship between time and speed, the efficiency of the system decreases to a minimum when the free fall velocity of about 33 m/s is reached. For this reason, to reach the desired efficiency level in MC-GES, it is recommended that the speed be below 10 m/s. Due to the relationship between speed and slope, it is necessary to avoid areas with steep slopes to prevent the cable car speed from increasing excessively owing to the effect of gravity. In inclined areas, electric motors can be used to control the speed of the cable car. [19,20].

3.5 Mountain Mine-Car solid gravity energy storage (MM-SGES)

AFEZMM-SGES consists of key components. These include weights, motor-generator units, cables, transmission fittings, rails and tilted surfaces. The system transforms electrical energy into gravitational potential energy. It works by moving weights between a high platform and a low platform. When there is a surplus of electricity, the engine pulls the minecart on the rails from the lower platform to the upper platform, while the weight rises and the potential energy increases. As the demand for electricity increases, the wagon on the upper platform is slowly lowered down and this movement produces electricity by causing the engine to rotate [21].

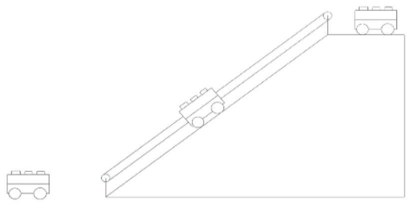

Fig. 3. Mountain Mine-Car solid gravity energy storage

This design was inspired by the use of PHES in places such as mountain slopes or old mines. The regenerative braking motor, which enhances the control and safety of the energy storage system, is located on the upper platform and is connected to the mining wagon by a cable. This technical route involves using gravel or concrete blocks to reduce high costs, and cables and rails that require high mechanical strength for transporting mine wagons [22]. The sloping ground must have a slope of approximately 6° to 25° for the mine wagon to operate efficiently; Too low a slope reduces efficiency, while too high a slope creates difficulties for the equipment [22]. MM-SGES and T-SGES systems have a similar modular structure and their energy storage capacities are comparable. However, the friction resistance of MM-SGES is higher compared to T-SGES.

4. APPLICABILITY ASSESSMENT OF SGES TECHNOLOGIES

In this section, the advantages and disadvantages of the application methods of SGES technology according to applicability factors are examined.

4.1 Tower solid gravity energy storage (T-SGES)

The T-SGES system has important advantages such as being able to be installed regardless of geographical limitations, shortening the construction process thanks to the rapid production of weight-bearing towers and blocks in a modular structure, and providing flexibility for different energy storage needs with its modular equipment structure. T-SGES has three shortcomings. Firstly, the mechanical strength of the material limits the load-bearing tower and the height of the tower is limited to 120 m, which affects the energy intensity. Secondly, the need to operate in a high-density environment leads to problems with equipment control and aging, resulting in reduced system safety. This situation is addressed to some extent by the EVRC design [12]. Lastly, Material use efficiency is reduced by some load-bearing blocks that are not used in the energy storage process.

4.2 Shaft solid gravity energy storage (S-SGES)

The main benefit of this technology is that it can achieve a significant height difference using existing mine shafts, offering a superior capacity compared to T-SGES systems, thanks to the full use of heavy loads. For S-SGES systems to respond quickly, weights must be kept in the mine shaft at all times. However, the disadvantages of this technology include excessive pressure and safety risks created by the support structure at the mine entrance. Additionally, the forced use of existing mine shafts increases the geographical limitations of S-SGES systems, and the cost of excavating new vertical shafts makes this technology not economically feasible [23]. Future improvements are hindered by the limited volumes of abandoned mines. This shows that SGES is ideal for small-scale energy storage and that hanging heavy loads for a long time increases energy consumption and reduces efficiency [16].

4.3 Piston solid gravity energy storage (P-SGES)

The main benefits of this technology include modularity and geographical adaptability; In this way, it does not require specific geographical conditions such as flat lands. However, favorable geographical conditions can significantly decrease structure costs. According to analyses conducted by Heindl Energy in 117 locations globally, 43% of these areas are buildable and 3% are quite suitable. Design and construction processes can be standardized, thus expanding the capacity of the storage facility. Thanks to the hydraulic systems' ability to react within seconds, P-SGES systems can regulate voltage and frequency and activate emergency services. However, the disadvantages of this technology include the high costs required to create artificial caves and the need for water resources. Compared to S-SGES, the energy density of P-SGES decreases by approximately 40% due to the buoyancy of water (the density of concrete is approximately 2.5 times that of water). Friction losses are unavoidable due to the piston structure. The whole system requires a high degree of sealing. That's why Heindl Energy uses geomembranes and concrete to seal natural rock fractures and recommends using a "rolling membrane" to keep water under high pressure under the piston; this method aims to reduce frictional losses between the piston and the wall. [24]

4.4 Mountain Cable-Car solid gravity energy storage (MC-SGES)

One of the prominent advantages of MC-SGES technology is that the energy storage system has excellent scalability and low heavy load cost, thanks to its modular structure. Additionally, thanks to the loading and unloading processes, heavy loads are not constantly loaded onto the carriers, allowing the carriers to be used more efficiently. However, this technology also has some disadvantages; for example, the presence of filling stations may reduce the effective height and overall efficiency of the system. Loading and unloading operations can cause equipment wear. In terms of geographical restrictions, it is more limited than MM-SGES and is especially suitable for geographical structures such as mountains and islands. [20]

4.5 Mountain Mine-Car solid gravity energy storage (MM-SGES)

The main advantages of MM-SGES technology are the expandability of the energy storage system thanks to its modular structure, low cost through the use of heavy materials such as gravel, and increased safety by eliminating the need for vertical hanging. According to the ARES report, the initial investment cost of this system is approximately 60% less per storage capacity compared to the PHES system. However, due to the large number of mechanical connections in the system, friction losses are high, which reduces efficiency. Outdoor working conditions can shorten the life of equipment and increase safety risks. It also requires sufficient height difference and large areas for land use, which requires high initial capital, especially in the absence of existing rails [25].

5. CONCLUSION AND DISCUSSION

Improving the efficiency of energy storage technologies plays a critical role in integrating theoretical knowledge with practical applications. Potential energy conversion is maximized, including the use of elastic potential energy to reduce the energy consumption of heavy loads, by optimizing engine power and transport routes. Integration of GES with electric grids requires the development of physical simulation models to analyze dynamic performance, allowing a better understanding of energy conversion processes and increasing efficiency. The successful implementation of GES projects is important for the integration of renewable energy sources and sustainable development. The development of energy storage methods compatible with renewable energy sources is of central importance in achieving future sustainable development purposes. Compared to other large-scale energy storage systems, SGES technology has significant advantages such as low geographical limitations, large storage volume, high energy conversion efficiency, long lifetime, low electricity generation cost, and high security. SGES is a novel and promising technology that has the potential to transform the current architecture of large-scale energy storage systems. However, there are some problems in existing research on SGES. The methods under certain conditions for the selection of different technical paths are unclear and more comprehensive techno-economic analyses are needed. Existing studies focus on existing technical pathways and show a lack of innovation in basic technologies. Optimal parameter design is still missing for some technical routes. Issues such as equipment inadequacy and the interactions of different technical means on the network require research.

REFERENCES

[1] Rahman, M. M., Khan, M. M. U. H., Ullah, M. A., Zhang, X., & Kumar, A. (2016). A hybrid renewable energy system for a North American off-grid community. Energy, 97, 151-160.

[2] Guney, M. S., & Tepe, Y. (2017). Classification and assessment of energy storage systems. Renewable and Sustainable Energy Reviews, 75, 1187-1197.

[3] EMEKSİZ, C., & Burak, K. A. R. A. (2022). Enerji Depolama Teknolojilerinin İncelenmesi ve Karşılaştırmalı Analizi. International Journal of Multidisciplinary Studies and Innovative Technologies, 6(2), 134-142.

[4] Rahman, M. M., Oni, A. O., Gemechu, E., & Kumar, A. (2020). Assessment of energy storage technologies: A review. Energy Conversion and Management, 223, 113295.

[5] https://thinktech.stm.com.tr/tr/enerji-depolama-teknolojilerindeki-son-gelismeler Accessed on 23 April 2024.

[6] Aydin, R. A., Baykal, Ş., Terciyanli, A., & Ertuğrul, Ç. A. M. (2020). Şebeke Seviyesinde Enerji Depolama Uygulamaları için Uygun Teknoloji Seçimi Metodolojisi Önerilmesi. Uluslararası Mühendislik Araştırma ve Geliştirme Dergisi, 12(3), 107-118.

[7] Mugyema, M., Botha, C. D., Kamper, M. J., Wang, R. J., & Sebitosi, A. B. (2023). Levelised cost of storage comparison of energy storage systems for use in primary response application. Journal of Energy Storage, 59, 106573.

[8] Kocaman, B. (2021). Enerji depolama teknolojileri

[9] Tong, W., Lu, Z., Chen, W., Han, M., Zhao, G., Wang, X., & Deng, Z. (2022). Solid gravity energy storage: A review. Journal of Energy Storage, 53, 105226.

[10] Moore, S. K. (2020). The Ups and Downs of Gravity Energy Storage: Startups are pioneering a radical new alternative to batteries for grid storage. IEEE Spectrum, 58(1), 38-39.

[11] He, W., King, M., Luo, X., Dooner, M., Li, D., & Wang, J. (2021). Technologies and economics of electric energy storages in power systems: Review and perspective. Advances in Applied Energy, 4, 100060

[12] Fyke, A. (2019). The fall and rise of gravity storage technologies. Joule, 3(3), 625-630

[13] Gravitricity renewable energy storage [EB/OL]. https://gravitricity.com/. Accessed on 29 April 2024

[14] O'Grady, C. (2021). Gravity powers batteries for renewable energy.

[15] GP. Gravity power – grid-scale energy storage, 2014. https://www.gravitypower. net/

[16] Li, F. F., Xie, J. Z., Fan, Y. F., & Qiu, J. (2024). Potential of different forms of gravity energy storage. Sustainable Energy Technologies and Assessments, 64, 103728

[17] Gravity Power LLC, GP Gravity Power, 2021. https://www.gravitypower.net/ Accessed on 23 April 2024

[18] Heindl Energy LLC, HE. Heindl Energy [EB/OL]. https://heindl-energy.com/ Accessed on 26 April 2024

[19] Yangyang, C., Hou, H., Xu, T., Wu, X., Liu, P., & Wang, H. (2019, December). A new gravity energy storage operation mode to accommodate renewable energy. In 2019 IEEE PES Asia-Pacific Power and Energy Engineering Conference (APPEEC) (pp. 1-5). IEEE.

[20] Hunt, J. D., Zakeri, B., Falchetta, G., Nascimento, A., Wada, Y., & Riahi, K. (2020). Mountain Gravity Energy Storage: A new solution for closing the gap between existing short-and long-term storage technologies. Energy, 190, 116419.

[21] Chen, K. (2022). Types, applications and future developments of gravity energy storage. Highlights in Science, Engineering and Technology, 3, 23-30.

[22] http://s3.amazonaws.com/siteninja/multitenant/assets/21125/files/original/All_About_ARES_-_070616.pdf Accessed on 26 April 2024

[23] Morstyn, T., Chilcott, M., & McCulloch, M. D. (2019). Gravity energy storage with suspended weights for abandoned mine shafts. Applied Energy, 239, 201-206.

[24] http://s3.amazonaws.com/siteninja/multitenant/assets/21125/files/original/All_About_ARES_-_070616.pdf Accessed on 21 April 2024

[25] Liu, X., & Li, K. (2020). Energy storage devices in electrified railway systems: A review. Transportation safety and environment, 2(3), 183-201